European Journal of Agronomy 154 (2024) 127061

Contents lists available at ScienceDirect

European Journal of Agronomy

journal homepage: www.elsevier.com/locate/eja

Modeling sugarcane development and growth within ECOSMOS biophysical model

Michel Anderson Almeida Colmanetti [a,*], Santiago Vianna Cuadra [b], Rubens Augusto Camargo Lamparelli [a], Osvaldo Machado Rodrigues Cabral [c], Daniel de Castro Victoria [b], José Eduardo Boffino de Almeida Monteiro [b], Helber Custódio de Freitas [d], Marcelo Valadares Galdos [e], Anderson Carlos Marafon [f], Aderson Soares de Andrade Junior [g], Sergio Delmar dos Anjos e Silva [h], Vinicius Bof Buffon [i], Thayse Aparecida Dourado Hernandes [j], Guerric le Maire [k,l]

[a] *Center of Energy Planning/University of Campinas, SP 13083-896, Brazil*
[b] *EMBRAPA Digital Agriculture, Campinas, SP 13083-886, Brazil*
[c] *EMBRAPA Environment, Jaguariúna, SP 13820-000, Brazil*
[d] *São Paulo State University, Bauru, SP 17033-360, Brazil*
[e] *Sustainable Soils and Crops, Rothamsted Research, Harpenden AL5 2JQ, United Kingdom*
[f] *EMBRAPA Coastal Tablelands, Rio Largo, AL 57100-000, Brazil*
[g] *EMBRAPA Mid-North, Teresina 64008-780, Brazil*
[h] *EMBRAPA Temperate Agriculture, Pelotas, RS 96001-970, Brazil*
[i] *EMBRAPA Cerrados, Brazilia, DF 73310-970, Brazil*
[j] *Brazilian Center for Research in Energy and Materials (CNPEM) - Brazilian Biorenewables National Laboratory, Campinas, SP 13083-100, Brazil*
[k] *CIRAD, UMR Eco&Sols, F-34398 Montpellier, France*
[l] *Eco&Sols, University of Montpellier, CIRAD, INRA, IRD, SupAgro, Montpellier, France*

ARTICLE INFO

Keywords:
Sugarcane
Process-based modeling
ECOSMOS

ABSTRACT

Sugarcane plays an important role in electricity and sugar production and is a viable biofuel. Developing and optimizing a mechanism that can predict crop growth and yield at different spatiotemporal scales can promote the understanding of the effects of cultivation on the ecosystem, while providing options for optimizing management measures and improving the operational procedures of sugarcane growers. The main objective of this study is to integrate the sugarcane module into the ECOSystem MOdel Simulator (ECOSMOS) model and calibrate a parameter set for sugarcane genotypes groups (using different datasets); the model supports datasets that vary in complexity (from flux tower experiments to operational plots), while accounting for high genotype-by-environment-by-management (GxExM) variability. First, we calibrated the ECOSMOS biophysical and physiological parameters for the sugarcane module using two micrometeorological experimental sites, based on eddy-covariance and biomass measurements. Second, sugarcane genotypes located in different regions of contrasting climate conditions were split into two groups based on their period of harvest, i.e., early or mid-to-late harvest season, and two parameter sets were proposed. The sugarcane module was used to estimate the yield of numerous plots, using two different parameter sets, namely, the general and regionally-specific parameter sets. The model could successfully simulate the biophysical and physiological processes of the biomass of stalks and leaves, energy and carbon fluxes, and soil-water dynamics; for Experimental Site 2, the Nash-Sutcliffe efficiency (NSE) was 0.14–0.86 and the relative root mean square error (RRMSE) was 13–112. However, the generic parameter set did not perform well in all production environments, and the difference between the observed and simulated yields ranged from 0.9 to 14.5 (Mg ha^{-1}). Hence, a novel calibration approach adopted in this study improved the module's accuracy, while improving the performances for all five production environments, with the difference between the observed and simulate yields being 0.3–2.2 (Mg ha^{-1}). Although the two parameter sets can be used as a reference for sugarcane plantations in Brazil, we recommend recalibrating the model (for ensuring higher accuracy) before operational applications. Notably, the ECOSMOS-sugarcane model is emerging

* Corresponding author.
E-mail address: michelcolmanetti@gmail.com (M.A.A. Colmanetti).

https://doi.org/10.1016/j.eja.2023.127061
Received 5 June 2023; Received in revised form 28 November 2023; Accepted 16 December 2023
Available online 5 January 2024

as a complex ecosystem model that can support the quantifications and evaluations of the effects of sugarcane plantations on the carbon and water balances in different environmental conditions, particularly in tropical regions.

1. Introduction

Reducing fossil-fuel consumption is one of the main aims for reducing greenhouse gas (GHG) emissions and thus, mitigate climate change (Tollefson, 2018). Biofuels are a relevant alternative renewable energy source that can be used to meet the energy demand while lowering GHG emissions (Daioglou et al., 2020, 2019). Sugarcane is a major crop for ethanol production; ethanol is obtained from sucrose fermentation. Additionally, electricity is generated from sugarcane bagasse burn; second-generation ethanol can be produced from sugarcane bagasse and straw, which can further increase the efficiency of sugarcane biomass utilization for energy purposes (Junqueira et al., 2017).

Given the importance of sugarcane in the scenario of the growing demand for alternatives to fossil-fuel energy sources, the area of sugarcane cultivation in countries like Brazil has increased in recent years (Hernandes et al., 2022). In the beginning of the 21st century, sugarcane plantations expanded from traditional growing regions to areas with different soils and climates, e.g., over the Brazilian Neotropical Savanna ("Cerrado" in Portuguese). The consequences of mechanical harvesting, e.g., soil compaction and physical damage to plants, have affected the regrowth vigor of plants in the region, leading to a reduction in their yields (Petrielli et al., 2023; Scarpare et al., 2015).

In this context, process-based crop models are important tools that can support the adoption of novel strategies and management practices, while minimizing loss and enhancing the yield. For example, the models can simulate hypothetical scenarios, predict plant growth in regions that are not generally used for the target crop, suggest the most suitable locations and periods for planting and harvesting, provide operational support, and, consequently, optimize yields. Several crop models, such as the Decision Support System for Agrotechnology Transfer for sugarcane (DSSAT-CANEGRO) and Agricultural Production Systems Simulator (APSIM-Sugarcane), are used for sugarcane growth and yield modeling (e.g., Dias and Sentelhas, 2017; Singels et al., 2014; Verma et al., 2023); this approach is feasible since these models have been developed and updated over decades. However, these models are generally limited to local scales, contrary to land surface models (LSM), such as the Joint UK Land Environment Simulator (JULES-crop; Vianna et al., 2022) and Agricultural version of the Integrated Biosphere Simulator (Agro-IBIS) model (Cuadra et al., 2012), which are applicable at regional and national scales and also are reasonable alternative models to understand the carbon and water balances in an ecosystem (above- and belowground) for different climate scenarios.

Although sugarcane is a robust tropical crop (i.e., it has a highly efficient C4 photosynthetic mechanism), Brazilian sugarcane plantations are located in contrasting conditions of hydrological and climatic stresses; therefore, making it a challenge to obtain a model that simulates plant growth and yield consistently across different environmental variabilities. The ECOSMOS model, which is based on the Agro-IBIS model, provides an effective agricultural ecosystem simulation framework (Foley et al., 1996; Kucharik et al., 2000); notably, it can simulate crop production and environmental impacts, e.g., the effects on carbon and water cycles. The model is composed of several modules, including a land surface module (Pollard and Thompson, 1995; Thompson and Pollard, 1995a, 1995b), biogeochemical module (Kucharik et al., 2000), and modules for natural vegetation and crops. Specific crop modules were developed for oil palm (Benezoli et al., 2021), eucalypt (Colmanetti et al., 2022), soybean and pasture (Dias et al., 2023), sugarcane (Cuadra et al., 2012), maize and wheat. The biophysical and physiological processes based on a land surface module linked to a crop simulation model dedicated to sugarcane render the ECOSMOS model the robustness to determine the sites in extensive regions of varying climate and soil type that can support sugarcane production.

This study aims to describe the sugarcane module implemented in the ECOSMOS simulation framework and present the results obtained from the calibration and evaluation processes. The specific objectives were to: (i) parametrize the ECOSMOS-sugarcane module using two monitored sites with flux towers; (ii) carry out calibration for two genotype groups (belonging to the early and mid-to-late harvest seasons) for contrasting climate and soil conditions; and (iii) assess the potential application of the module for estimating the yield of commercial sugarcane plantations in different production environments.

2. Material and methods

2.1. Model descriptions: ECOSystem MOdel Simulator for sugarcane (ECOSMOS-sugarcane)

The ECOSMOS model serves as a framework for energy and mass balance simulations and can consider two canopy levels. The core physical code of the simulator is derived mainly from the IBIS and Agro-IBIS models (Foley et al., 1996; Kucharik and Brye, 2003). ECOSMOS is a modularized simulation framework written in C+ + and includes modules dedicated to the biogeochemical cycle, plant physiology, radiation balance, and crop growth (every crop has its own module). In previous studies, the energy, water, and carbon exchanges between soil, vegetation (canopy and root system), and atmosphere were calculated using the LSM at hourly time steps (Pollard and Thompson, 1995; Thompson and Pollard, 1995a, 1995b). The C3 and C4 photosyntheses were calculated as the minimum of three potential capacities to fix carbon, following the Farquhar equations (Farquhar et al., 1980); and stomatal conductance was calculated based on the original Ball–Berry–Leuning (BBL) model (Leuning, 1995; Miner et al., 2017) and/or the updated BBL equation by (Cuadra et al., 2021).

In this model, the hydrological processes simulate precipitation interception and water retention by the canopy, surface puddle formation, infiltration, water flux through soil layers, deep percolation, evaporation from the soil surface and water intercepted by the canopy, and canopy transpiration. The number and size of soil layers can be set up, and the model simulates the hourly heat and water flux through the soil profile. The soil-water flux was calculated using Richard's equations for saturated and unsaturated water flows (Farthing and Ogden, 2017). The soil hydraulic properties can be completely described or estimated using pedotransfer functions (PTF), in accordance with Tomasella et al. (2000). The runoff equations follow the United States Department of Agriculture Soil Conservation Service's (USDAS-CS's) empirical rainfall-runoff model (USDA-SCS, 1998).

In a previous study, the decomposition of soil organic matter was simulated by the biogeochemical module, which was based on the "Century" model with a daily time-step (Kucharik et al., 2000). Notably, the rates of litter decomposition and microbial biomass turnover depend on soil temperature and moisture, with an average of 0–10 cm for litter and 0–100 cm for microbial biomass (Kucharik et al., 2000).

The ECOSMOS-sugarcane module (Fig. 1) used in this study was mostly based on the equations (Eqs. 1–16) presented by Cuadra et al. (2012), which were developed using two widely used sugarcane crop models, APSIM-Sugarcane (Keating et al., 1999) and CANEGRO (Singels et al., 2005; Singels and Bezuidenhout, 2002) and previously implemented in the Agro-IBIS model. The module allocates the net primary production (NPP), as a function of the growing degree days (GDDs), to

four plant component pools: leaves, roots, stalk-structural (fiber and non-sucrose materials), and stalk-sucrose (sugar as sucrose). Relative maturity (RM), which refers to the summation of the GDD along the cycle normalized by the total GDD to reach physiological maturity, was used in the model as the temporal scale to drive the allocations.

The RM [%; Eq. (1)] expresses the changes in the GDD along the sugarcane lifespan on a scale from 0 to 100.

$$RM = 100 * \left(\frac{GDD_n}{GDD_m}\right) \quad (1)$$

$$GDD_n = GDD_{n-1} + \left(\frac{T_{\max} - T_{\min}}{2} - T_{base}\right) \quad (2)$$

where GDD_m is the reference value for the GDD in the maturity age (K); GDD_n is the GDD at day n; $T_{\max}$ and $T_{\min}$ are the maximum and minimum temperature (K) for day n, respectively; and T_{base} is the minimum threshold value of the temperature required for plant development (K).

The value of heat unit index (HUI_{leaf}), which refers to the value of GDD (K) (after planting) necessary for leaf emergence, was calculated using Eq. (3).

$$HUI_{leaf} = GDD_m * Leaf_{emerg} * E_f \quad (3)$$

where $Leaf_{emerg}$ is the parameter that regulates leaf emergence (dimensionless), and E_f is the factor for reducing the emergency development for sugarcane plant (dimensionless, 1 for the first growing year and 0.2 for sugarcane ratoons).

When $GDD_n > HUI_{leaf}$, sugarcane begins accumulating biomass, and the daily net carbon assimilated along the day is allocated to different plant organs. First, the model computed the fraction of the NPP allocated to the aboveground components, which was calculated based on the coefficient of allocation, $Coef_a$ (dimensionless), as shown in Eq. (4) below:

$$Coef_a = (1 - Coef_{roots\_\min}) * \min[1, 1 - e^{-(R_d * RM * P_f)}] \quad (4)$$

where $Coef_a$ is the allocation coefficient for the aboveground carbon components (stalk and leaves; ranging between 0 and 1); $Coef_{roots\_\min}$ is the minimum allocation coefficients to roots (ranging between 0 and 1); R_d is the root decline parameter; and P_f is the factor for reducing the aboveground development parameter (which was 0.6 for sugarcane in the growing year and 1 for ratoons).

Then, the $Coef_a$ was split between stalk and leaves. The stalk allocation coefficient, $Coef_{stalk}$, was calculated using Eq. (5). Notably, F_1 [calculated using Eq. (6)] and F_2 [calculated using Eq. (7)] are the linear and logarithmic functions that describe the fraction of the aboveground carbon that gets allocated to the stalk initially and for most of the plant lifespan, respectively.

$$Coef_{stalk} = \min[(1 - Coef_{leaves\_\min} - Coef_{roots\_\min}), Coef_a \quad * \max(0, F_1, F_2)] \quad (5)$$

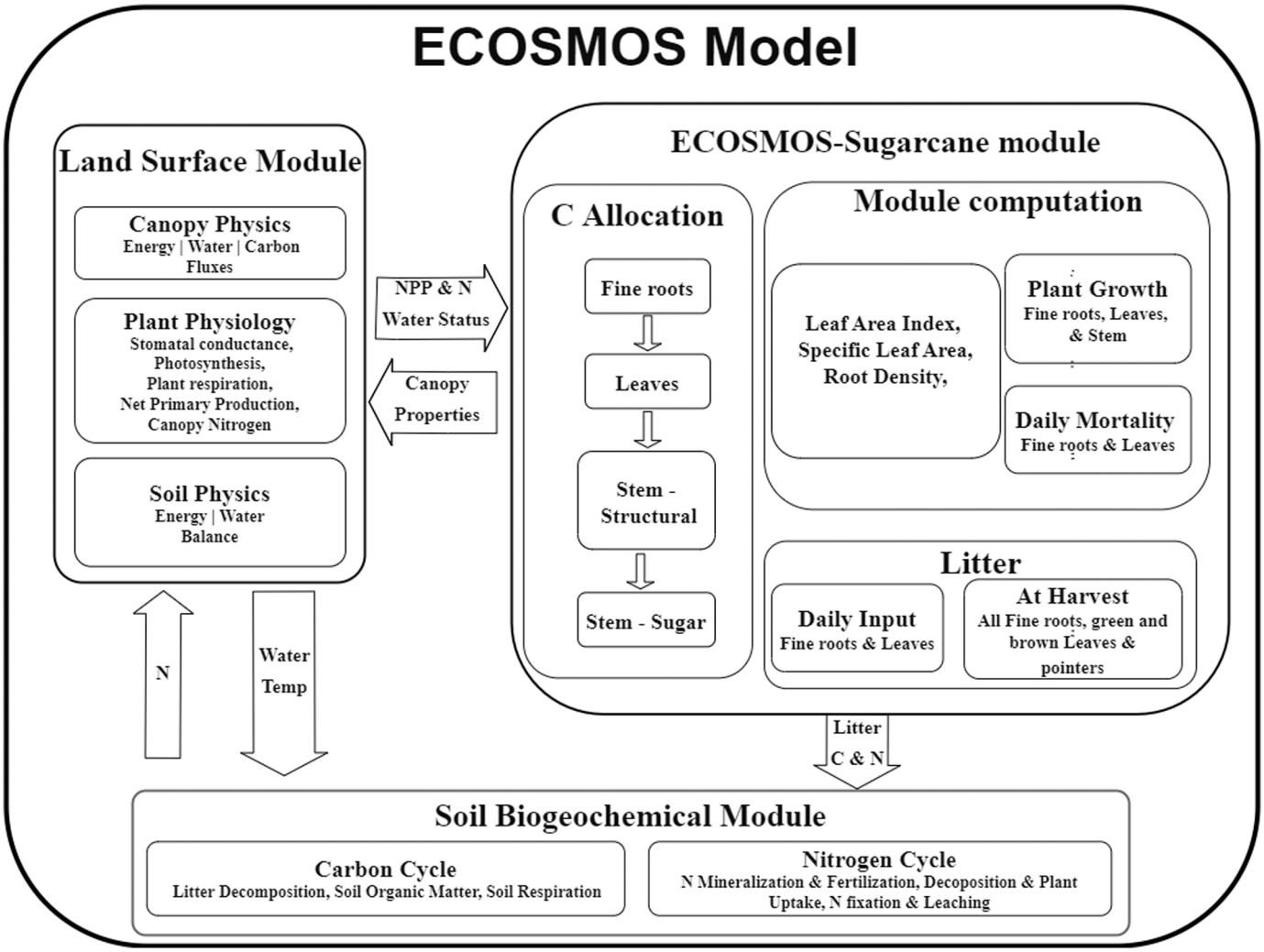

Fig. 1. Schematic representation of the ECOSystem MOdel Simulator (ECOSMOS)-sugarcane model employed in this study.

$$F_1 = \max(0, (RM * C_{lstalk}) - (I_{lstalk} * C_{lstalk})) \quad (6)$$

$$F_2 = \max(0, \left(1 - e^{[(RM*C_{estalk})-(I_{estalk}*C_{estalk})]}\right)) \quad (7)$$

where $Coef_{stalk}$ ranges between 0 and 1; $Coef_{leaves\_min}$ and $Coef_{roots\_min}$ are the minimum allocation coefficients (and ranging between 0 and 1) to the leaves and roots, respectively; C_{lstalk} and I_{lstalk} are the parameters that define the linear carbon allocation to the stalk at the beginning of stalk growth; and C_{estalk} and I_{estalk} are the parameters that define the logarithmic growth of carbon allocation to the stalk, with the allocation for most of stalk development period being dominant.

The leaf allocation coefficient, $Coef_{leaves}$, which ranged between 0 and 1, was calculated using Eq. (8).

$$Coef_{leaves} = Coef_{a} – Coef_{stalk} \quad (8)$$

Then, we calculated the fraction of stalk that was considered to be sucrose (referred to as "stalk-sucrose"). The stalk-sucrose allocation coefficient, $Coef_{suc}$, calculated using Eq. (9), ranged between 0 and 1. As shown in Eqs. (10) and (11), F_3 (Eq. 10) and F_4 (Eq. 11) are the linear (dominating in the beginning of stalk growth) and logarithmic functions that describing the fraction of the aboveground carbon that goes to the stalk-sucrose, respectively. They are responsible for the allocation for most of plant lifespan.

$$Coef_{suc} = Coef_{stalk} * \max(0, F_3, F_4) \quad (9)$$

$$F_3 = \max(0, (RM * C_{lsuc}) - (I_{lsuc} * C_{lsuc})) \quad (10)$$

$$F_4 = \max(0, \left(1 - e^{[(RM*C_{esuc})-(I_{esuc}* C_{esuc})]}\right)) \quad (11)$$

where C_{lsuc} and I_{lsuc} are the parameters that define the carbon allocation to the stalk-sucrose of F_3, and C_{esuc} and I_{esuc} are the parameters when the logarithmic function F_4 allocates carbon to the stalk-sucrose.

The carbon allocated to the stalk-structural was calculated using $Coef_{struc}$, as show in Eq. (12) below:

$$Coef_{struc} = Coef_{stalk} – Coef_{suc} \quad (12)$$

The root allocation coefficient, $Coef_{roots}$, was calculated using the Eq. (13) below:

$$Coef_{roots} = 1–\mathrm{Coef_a} \quad (13)$$

The leaf area index (LAI; m^2 m^{-2}) was calculated using Eq. (14) below:

$$LAI = (C_l * SLA) \quad (14)$$

where C_l is the current amount of carbon in the leaves compartment (kg C m^{-2}), and SLA is the specific leaf area (m^2 kg^{-1}).

The $LAI_{Intercept}$ [calculated using Eq. (15)] is the effective LAI that intercepts light; it depends on the total green LAI (LAI_g) and is a relative fraction of dead leaves (LAI_b), parameterized through a coefficient of interception of dead leaves (IDL). The radiation IDL is a coefficient that reduces the relative fraction, with respect to the green leaves and the area projected in the incident radiation plane, as dead leaves have smaller inclination angle and are usually located bellow green leaves. Dead leaves have a direct impact on light interception, calculated by altering the green fraction of the canopy, $Greefrac$ [see Eq. (16)]. $Greefrac$ impacts the gross primary production (GPP) directly, as only the fraction of photosynthetically-active radiation (PAR) absorbed by green leaves can be accounted for photosynthesis.

$$LAI_{Intercept} = LAI_g + LAI_b * IDL \quad (15)$$

$$Greefrac = \frac{LAI_g}{LAI_{Intercept}} \quad (16)$$

After calculating all the allocation coefficients, they were multiplied by the NPP to obtain the carbon allocated for each component (stalk-structural, stalk-sucrose, leaves, and roots).

Leaf mortality was computed on a daily basis, while considering the fact that the dead leaves do not fall immediately after their mortality but stay attached to the stalk after senescence; thus, they were computed only with respect to litterfall (after the harvest). The dead root mass was computed daily; notably, dead root mass is generally regulated by the total roots in the soil layer and the root turnover rate. The soil biogeochemical module accounted for the carbon cycle up to soil depth of 1 m; therefore, only the fraction of dead roots up to the depth of 1 m was included in the soil carbon model. Note that sugarcane roots can grow deeper than 1 m, and the model accounts for the water absorption bellow 1 m; the soil water module is independent of the biogeochemical module containing different soil layers of different sizes. Additionally, after the harvest of each rotation, we assumed that the leaf mortality was 17% of the roots (Ball-Coelho et al., 1992). The daily stalk mortality was not computed. At harvest, the leaves and the top of the stalk immediately add to the surface litter, while the roots experience a period of senescence, eventually becoming a part of soil letter.

For this study, the ECOSMOS module was implemented in a framework that supported multiple programming languages (most of the code was in C+ +), however some modules were in Fortran, to benefit from the computational performance of C+ + and its flexibility.

2.2. Field dataset descriptions

Sugarcane is a semi-perennial crop planted and harvested after 12–18 months. The first year refers to the growing year when the sugarcane is first planted in the field, and ratoon sugarcane refers to when the sugarcane sprouts from the previously harvested ratoon. In this study, four datasets were used for parameterization/evaluation and calibration/evaluation for different growing-year lengths (12–18 months) and different numbers of ratoons.

Dataset 1 consisted of two highly monitored experimental sites, including the eddy-covariance measurements of carbon and water fluxes between the ecosystem and atmosphere. One site was used for parameterization (Site 1) and the other for evaluation (Site 2). Dataset 2 consisted of a set of experimental sites having multiple sugarcane varieties; these sites had different climatic conditions and soil textures. Dataset 3 consisted of several commercial sugarcane plantations located in the State of Goiás (Brazil), with each plantation having different soil hydraulic properties and production environment. The last dataset was used to verify the model performance, based on the calibration obtained using Dataset 2 (with respect to crop yield). Fig. 2 illustrates the distribution of the sites considered in this study, and Table 1 describes the level of information for each dataset.

2.2.1. Dataset 1

Dataset 1 (Fig. 2) consisted of sites 1 and 2. Site 1 is located at Pirassununga, São Paulo State (21°57' S, 47°20' W; altitude = 657 m). The region is characterized by the Cwa climate (Humid Subtropical, with dry winter and hot summer), with an average annual rainfall of 1410 mm and average annual temperature of 22 °C. The soil classification was oxisol with clay texture. The IAC SP 95–5000 genotype was planted in 2015, and the observed period corresponded to the growing year and the period of 2015–2018, when two consecutive ratoons sprouted. A flux tower (9 m) was installed in October 2015, 23 days after planting. The H_2O and CO_2 fluxes were obtained using an eddy covariance system (Cabral et al., 2020) equipped with a three-dimensional sonic anemometer (CSAT3) and an infrared H_2O/CO_2 analyzer (EC150), both being manufactured by Campbell Scientific, Inc. in Logan (Utah, USA). Radiation sensors (Kipp & Zonen, Delft, The Netherlands) were installed at the top of the flux tower, to monitor the components (incident and reflected) of global solar radiation (Rg), PAR, and net radiation (Rn). Other measurements included air temperature and humidity using Vaisala's HMP45 sensor (Helsinki, Finland) in a forced ventilation shelter; the total precipitation was measured using TB4 rain

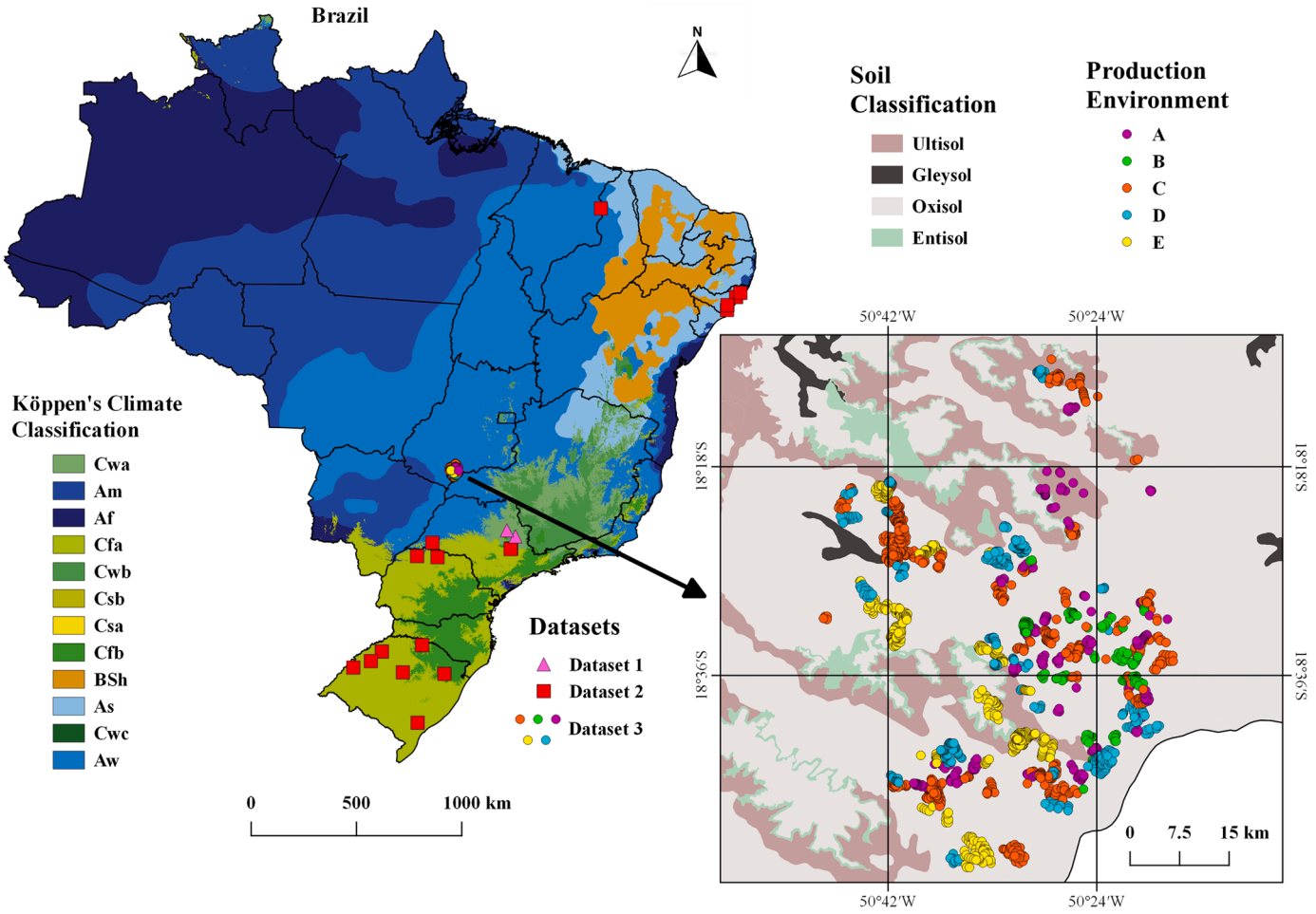

Fig. 2. Experimental sites and sugarcane field plots used for the parametrization, calibration, and evaluation for the ECOSystem MOdel Simulator (ECOSMOS)-sugarcane model. A detailed description of Datasets 1, 2, and 3 is given in Section 2.2, based on the Köppen climate classification according to Alvares et al. (2013).

gage (Hydrological Services Pty. Ltd., New South Wales, Australia). Soil moisture was measured using reflectometers (CS615, Campbell SI, Logan, Utah, USA) installed vertically (0.3 m layers) on the ground surrounding the tower (to the soil depth of 2.7 m). Biomass sampling was performed every 30 d (Fig. 3), and sampling was carried out randomly at 10 points. The full aboveground biomass was harvested in 2 m linear, where the green biomass of green and dry leaves and stalks were weighed. A subsample of each biomass component was obtained to determine the dry biomass content in each sample using a forced ventilation oven (70 °C), with measurements being carried out until a constant weight was achieved.

Site 2 was located in Luiz Antonio, São Paulo State (21°38' S, 47°47' W; altitude = 552 m). The region was classified as Cwa (Humid Subtropical, with dry winter and hot summer), with an annual rainfall of 1440 mm and average temperature of 23 ºC. The soil classification type was oxisol with sandy clay-loam texture. The planting (SP83–2847 genotype) was carried out in 2004, with the spacing between the rows being 1.5 m. The flux tower (8.5 m) was installed in early February of 2005, and the period of measurements corresponded to the second and third ratoons during 2005–2007. The H_2O and CO_2 flows (Cabral et al., 2013, 2012) were obtained by an eddy covariance system, using a sonic anemometer (R2, Gill Inst., Lymington, Hampshire, UK) and a closed-path infrared gas analyzer (IRGA, LI6262, Li-Cor Biosciences, Lincoln, Nebraska, USA). The incident and reflected solar radiation (Rg), PAR, and Rn were measured using Kipp and Zonen sensors (Delft, The Netherlands); the air temperature and humidity were measured using CSI HMP45C (Campbell SI, Logan, Utah, USA), and the precipitation was measured using TB4rain gage (Hydrological Services Pty. Ltd. New South Wales, Australia). Soil moisture was monitored using 10 reflectometers (CS615, Campbell SI, Logan, Utah, USA) installed vertically (0.3 m layers) at the soil depth of 2.7 m. Biomass sampling was performed at 10 random sampling points in the plantation site, every 20–30 d. At every sampling point, the number of stalks in 2 m of row were counted; a total of five stalks were sampled (one at every 0.4 m). The biomass fractions were separated (green leaves, dry leaves, and stems) and the dry mass was determined using the subsamples of each fraction (10%), after drying the samples in a forced ventilation oven (70 °C) until the samples reached constant weights.

2.2.2. *Dataset 2*

The 18 sites of Dataset 2 were located in regions with different climate and soil texture (Fig. 3 and Table 1). Nine sites were classified as Cfa (Humid subtropical oceanic climate, without dry season and with hot summer); three sites were classified as As (Tropical with dry summer), two as Cfb (Humid subtropical Oceanic climate without dry season with temperate summer), two as Cwa (Humid Subtropical with dry winter and hot summer), one as Am (Tropical monsoon), and one as Aw (Tropical with dry winter). Complete biometric data (stalk, leaves, LAI and/or yield data) was available for eight sites; for 10 of these sites, only the yield data was available. The predominant genotypes of the crop were RB855156, RB966928, RB867515, and RB92579. For three sites, only the biometric and/or yield data for the growing year were available: for 14 sites, only the data for the growing year and ratoons were available. The data for soil physical properties, such as texture, field

Table 1
Summary of the datasets used for the parameterization, calibration, and evaluation of the ECOSystem Model Simulator (ECOSMOS)-sugarcane model.

Dataset	Site Number	Coordinates	Climate	Soil Texture	Genotype	Level of information
1	1	21°57'S, 47°20'W	Cwa	Clay	IAC SP95-5000	Flux Tower; Stalk, Leaves & LAI
	2	21°38'S, 47°47'W	Cwa	Sandy Clay Loam	SP83-2847	Flux Tower; Stalk, Leaves & LAI
2	3	31°40'S, 52°26'W	Cfa	Clay Loam	RB855156, RB867515, RB92579 & RB966928	Stalk, Leaves, LAI & Yield
	4	22°59'S, 52°28'W	Cfa	Sandy Clay Loam	RB036066, RB867515 & RB966928	Stalk, Leaves, LAI & Yield
	5	23°2'S, 51°24'W	Cfa	Sandy Clay Loam	RB855156 & RB867515	Stalk, Leaves & LAI
	6	22°17'S, 51°40'W	Cfa	Clay	RB855156 & RB867515	Stalk, Leaves & LAI
	7	9°28'S, 35°50'W	As	Sandy Loam	SP79-1011, RB92579, RB931530 & RB93509	Stalk, Leaves, LAI & Yield
	8	10°9'S, 36°18'W	As	Sandy Loam	RB92579	Stalk, Leaves, LAI & Yield
	9	22°35'S, 47°34'W	Cwa	Clay	RB966928	Stalk & Yield
	10	22°37'S, 47°35'W	Cwa	Clay	IACSP-5000	Stalk & Yield
	11	4°51'S, 42°53'W	Aw	Sandy Loam	RB867515, RB863129, RB72454, RB921011, RB931530, RB92579, RB962962, RB98710, SP79-1011 & VAT90212	Yield
	12	29°8'S, 51°3'W	Cfb	Clay Loam	RB855156, RB966928 & RB867515	Yield
	13	27°38'S, 52°12'W	Cfb	Sandy Clay	RB855156, RB966928 & RB867515	Yield
	14	27°57'S, 54°18'W	Cfa	Clay Loam	RB855156, RB966928 & RB867515	Yield
	15	29°3'S, 53°12'W	Cfa	Sandy Clay	RB855156, RB966928 & RB867515	Yield
	16	27°57'S, 54°18'W	Cfa	Sandy Clay	RB855156, RB966928 & RB867515	Yield
	17	28°48'S, 55°48'W	Cfa	Sandy Clay Loam	RB855156, RB966928 & RB867515	Yield
	18	28°27'S, 54°53'W	Cfa	Clay	RB855156, RB966928 & RB867515	Yield
	19	9°15'S, 35°36'W	Am	Loamy Sand	RB92579	Yield
	20	9°54'S, 36°17'W	As	Loamy Sand	RB92579	Yield
3	21 - 234 (Prod. Env. A)	18°53'S - 18°9'S, 50°17'W - 50°48 W	Aw	Clay	Not Available	Yield
	235 - 373 (Prod. Env. B)			Clay Loam		Yield
	374 - 976 (Prod. Env. C)			Sandy Clay Loam		Yield
	977 - 1335 (Prod. Env. D)			Sandy Clay Loam		Yield
	1336 - 1759 (Prod. Env. E)			Loamy Sand		Yield

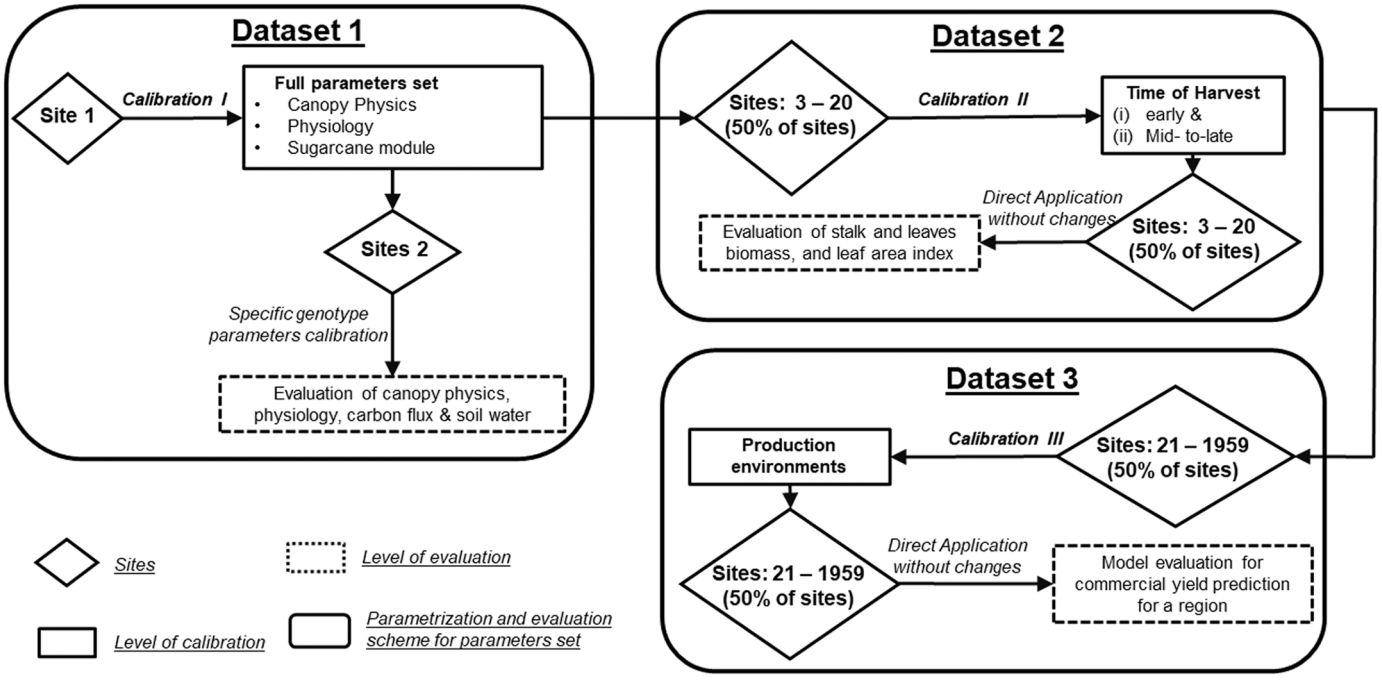

Fig. 3. Schematic representation of the parametrization, calibration, and evaluation of the new ECOSystem MOdel Simulator (ECOSMOS)-sugarcane module employed in this study.

capacity, and permanent wilting point, were available for all the sites. Notably, the majority of sites considered in this study belong to an experimental network coordinated by the Brazilian Agricultural Research Corporation (EMBRAPA). The data for sites 7 and 8 are available online (Barbosa et al., 2021); sites 11 and 12 were part of the project Sugarcane Renewable Electricity (SUCRE; Souza et al., 2021).

2.2.3. Dataset 3

Dataset 3 was composed of 1739 sugarcane fields (management units) located in Quirinópolis, Goiás State, Brazil. The region was classified as Aw (Tropical savanna with dry winter), with an annual rainfall of 1400 mm and average temperature of 23 °C. The soils were classified as Oxisol, Ultisol, Entisol, and Gleysol. The sugarcane fields were distributed in five different production environments, namely, A, B C, D and E. The production environments were management zones classified according to the chemical properties and water-holding capacity of the soil. As a consequence of the difference in nutrients and water availability, the production environments led to different rooting depths, with Environment A having the deepest and Environment E having the shallowest rooting depth. The information for specific genotypes for each sugarcane field were not available; however, overall, more than 40 genotypes were distributed among the fields. For sugarcane fields, the data is composed of fields with only the growing year (664 fields), growing year and one ratoon (814 fields), and growing year and two ratoons (261 fields), a total of 1739 fields. The sugarcane production in these fields was carried out between 2016 and 2019. Sugarcane was mechanically harvested, with crop residues (leaves and shoots) left in the field, and only the stalks transported to and processed by the industry for sugar, ethanol, and electricity production.

The sugarcane harvesting season lasted for 7–9 months in the dry season. The harvesting sequence was driven by two main parameters: 1) Production environment: As water deficit increased toward the mid-to-late harvesting season, the fields under production environments D and E, which had the lowest soil-water holding capacity, were harvested first, and those under production environments A and B were harvested later, to minimize yield loss. 2) Genotype susceptibility to water deficit and their precocity to accumulate stalk sucrose (according to ripening precocity): Breeding programs traditionally classify genotypes into three ripening groups: early, medium, and late harvest seasons. In this study, the genotypes were grouped into early and mid-to-late harvest seasons, a classification commonly adopted by farmers.

2.3. Parametrization, calibration, and evaluation procedures

The three datasets were used for parameterization/evaluation and calibration/evaluation of the ECOSMOS-sugarcane module. A schematic representation is shown in Fig. 3. Sites 1 and 2 (Dataset 1) contained a flux tower; therefore, they were used for the parametrization of the biophysical and physiological processes of the plant, e.g., photosynthesis, stomatal regulation, and radiation fluxes, with the initial parameter values obtained from previous studies (Cuadra et al., 2021, 2012; Kucharik et al., 2000). Model parametrization was obtained through a series of simulations, wherein the parameters varied to pre-defined intervals. A hierarchical structure of parametrization was performed, while adhering to the following sequence: by adjusting the (i) radiation interception and absorption, (ii) soil-water retention and water fluxes, (iii) physiological processes related to photosynthesis and evapotranspiration, and (iv) carbon allocation and plant mortality.

The largest number of in-situ measurements were carried out for Site 1; thus, the site was used for model parametrization. Site 2 was used to evaluate the results. The parameter sets obtained for Site 1 was used for Site 2; however, two parameters (namely, specific leaf area and rooting profile) were adjusted to account for the different genotypes grown in the sites. The parameter sets are available in the Supplementary Material (Table S1).

Dataset 2 was used to calibrate the ECOSMOS-sugarcane module according to the variable genotype-by-environment (GxE), to obtain two generic parameter sets for the early and mid-to-late maturity genotypes, hereafter referred to as EMG and MLMG (Table S1), respectively. A total of 41 simulations were performed for Dataset 2 (from Site 3 to Site 20), corresponding to the combination of sites and genotypes. The simulations were split into two subsets based on the genotypes, as follows: (i) early harvest season maturity group (i.e., genotypes CTC9001, CTC9003, RB855156, RB855453, RB863129, RB931530, RB966928, and RB98710), and (ii) mid-to-late harvest season maturity group (i.e., genotypes CTC2, CTC963346, IACSP955000, RB036066, RB72454, RB867515, RB921011, RB92579, RB93509, RB962962, SP791011, SP801816, SP832847, and VAT90212). For each subset, half of the simulations were randomly selected (subset 1) and used for calibration, and the other half (subset 2) was used for evaluation. For each subset, we performed the same number of simulations, with similar biometrics and/or yield-level information, or with only the yield information. The full parametrization obtained for Site 1 was maintained for the majority of the parameters, and only a few parameters dedicated to the ECOSMOS-sugarcane module were re-calibrated; these parameters were leaf emergency, thermal time, maximum LAI, specific leaf area, and root and leaf allocation parameters.

Dataset 3 was used to evaluate the calibration obtained from Dataset 2 and also to carry out an additional calibration that was adjusted to one farm group. Datasets 2 and 3 portrayed large GxE variability, but Dataset 3 differed from Dataset 2 with respect to the management process. While Dataset 2 consisted of experimental sites that adopted standardized agricultural management, Dataset 3 was limited to operational field plots, wherein farm management had significant influence on crop yield. As no genotype information was available for Dataset 3, we assigned the parameter set of the early harvest season to the sugarcane fields harvested before 31st of July; for the plantations harvested after this period, we used the parameter sets of the mid-to-late harvest season. A third calibration was performed to maximize the module performance for simulating the crop yield, referred to as “Farm calibrations” (Farm-EMG and Farm-MLMG; Table S1), while accounting for the effects of management on the yield.

Similar to Dataset 2, Dataset 3 was split into two subsets as well, with half of the simulations being selected (subset 1) randomly and used for calibration, and the other half (subset 2) being used for evaluation, based on five production environments (i.e., A, B, C, D and E). For recalibration, the plots classified into production environment B were used as reference, once those had the higher yield. The set of parameters related to the sugarcane module adjusted for predicting the yield for environment B was maintained for the simulations of the plots classified into production environments A, C, D and E. For predicting the yields for the environments A, C, D and E, we changed and reduced the potential root depth and soil water retention. With respect to root density, for production environments C and D, approximately 95% (of the total roots) was observed in the top 40 cm of the soil profile; for production environment E, approximately 95% was noted in the top 30 cm of the soil profile.

2.4. Simulation settings

For Dataset 1, we used hourly meteorological data to run the model at an hourly time-step. For datasets 2 and 3, the daily meteorological data (precipitation, maximum and minimum temperature, solar radiation, relative humidity, and wind speed) were obtained locally or from external sources (Xavier et al., 2022). Diurnal cycles were synthetically generated using the original IBIS functions (Foley et al., 1996). The soil physical and hydraulic properties used by the model were soil total porosity (volume fraction), field capacity (volume fraction), wilting point (volume fraction), Campbell’s “b” exponent (for computing the unsaturated soil water fluxes), saturated hydraulic conductivity (m s^{-1}), and granulometric fractions for each soil layer. When the data of the saturated and drained upper limits and the lower limit of plant

extractable water were not available, we used a PTF (Tomasella et al., 2000). For estimating the saturated hydraulic conductivity of the soil, we used the functions proposed by Tomasella and Hodnett (1997). For soil-water content initialization, the timeline of the simulations began a year before the planting date.

2.5. Model evaluation

For Dataset 1, the Nash-Sutcliffe efficiency (NSE) [see Eq. (17)] was used to evaluate the prediction of Rn, net ecosystem exchange (NEE), GPP, evapotranspiration (ET), LAI, and biomass. The same analysis was performed for assessing the biomass of datasets 2 and 3, depending on data availability. Additionally, we calculated the relative root mean square error (RRMSEs) [Eq. (18)] and mean biases (MBs) [Eq. (19)] for all the variables.

$$NSE = 1 - \frac{\sum_{i=1}^{n}(a_i - \widehat{a}_i)^2}{\sum_{i=1}^{n}(a_i - \overline{a}_i)^2} \quad (17)$$

$$RRMSE = \frac{\sqrt{\frac{\sum_{i=1}^{n}(\widehat{a}_i - a_i)^2}{n}}}{\frac{\sum_{i=1}^{n} a_i}{n}}.100 \quad (18)$$

$$MB = \frac{\sum_{i}^{n}(\widehat{a}_i - a_i)}{n} \quad (19)$$

where a_i denotes the observed values; $\widehat{a}_i$ denotes the simulated values; and n is the number of observations.

For Dataset 1, we carried out non-parametric local regression (LOESS), with 95% confidence interval and SPAN value of 0.1 (for a fraction of the data points used to fit the model), for NEE, ET, Rn, GPP, and Volumetric Water Content (VWC). The VWC is defined as the ratio of the volume of water to the unit volume of soil ($m^3\ m^{-3}$). The confidence intervals that overlap the predicted and observed values of NEE, ET, Rn, and VWC indicated non-statistical differences along the time series. The GPP vs Air Temperature (C°) and GPP vs humidity (%) were graphically analyzed by plotting the quantile of 100% of GPP (to express the maximum values against both the variables). The paired t-test with 95% confidence interval was performed (for the yield), to compare the statistical difference between the means of the observed and simulated data. The Wilcoxon signed-rank test was used as an alternative for data with no Gaussian distribution for residues. The potential water available (PAW) is the maximum amount of water stored in a soil profile that can be used by plants. In this study, the PAW was normalized between 0 and 1, representing the absence of water available for plants and the maximum capacity of water use by plants, respectively. A graphical analysis of PAW was also performed for sites 1 and 2. The analyses were performed using R R Core Team (2020).

3. Results

3.1. Evaluation of the ECOSystem MOdel Simulator (ECOSMOS)-sugarcane model

The ECOSMOS-sugarcane model consistently simulated (with high positive values of NSE and low values of RRMSE and MB, Table 2) the Rn, GPP, NEE, ET, and soil water content (Figs. 4–6) for sites 1 and 2. This indicated that the model could successfully carry out the parameterization and evaluation for sites 1 and 2, respectively.

Despite the individual performance of each variable, the model precisely followed the observed seasonality pattern for Rn, NEE, and ET. The variables Rn, NEE, and ET fluctuated along the simulation period (Figs. 4 and 5), with the highest values of NEE (expressed negatively), Rn, and ET being noted in summer, a period with accentuated crop growth, and lower values being noted in the post-harvest period (characterized by the predominance of belowground plant metabolic). The highest positive values of NEE were noted during the periods of litterfall and decomposition (Figs. 4 and 5).

Table 2
Performance of the ECOSystem MOdel Simulator (ECOSMOS) model for different variables for the two experimental sites considered in this study (Dataset 1). Abbreviations: net radiation (Rn); gross primary production (GPP); net ecosystem exchange (NEE); evapotranspiration (ET); leaf area index (LAI); dry matter (DM); Nash-Sutcliffe efficiency (NSE); relative root mean square error (RRMSE); mean bias (MB).

Dataset	Site	Variables	Units	NSE	RRMSE	MB
1	1	Stalk	kg DM m^{-2}	0.89	24.21	-0.11
		Leaves	kg DM m^{-2}	0.58	30.03	-0.05
		LAI	$m^2\ m^{-2}$	0.67	26.34	-0.07
		Rn	W m^{-2}	0.89	10.74	0.65
		GPP	g C m^{-2} day^{-1}	0.37	109.20	2.70
		NEE	g C m^{-2} day^{-1}	0.03	90.93	-1.80
		ET	mm day^{-1}	0.54	30.82	-0.11
		WVC (0-2.7 m)	$m^3\ m^{-3}$	0.75	3.78	-0.01
		PAW (0-2.7 m)	Dimensionless	0.62	35.29	-0.03
	2	Stalk	kg DM m^{-2}	0.86	45.53	-0.03
		Leaves	kg DM m^{-2}	0.65	43.88	0.03
		LAI	$m^2\ m^{-2}$	0.62	45.46	0.36
		Rn	W m^{-2}	0.72	23.26	1.81
		GPP	g C m^{-2} day^{-1}	0.52	112.42	2.20
		NEE	g C m^{-2} day^{-1}	0.14	99.29	-1.58
		ET	mm day^{-1}	0.61	39.39	0.58
		WVC (0-2.7 m)	$m^3\ m^{-3}$	0.47	13.15	0.01
		PAW (0-2.7 m)	Dimensionless	0.49	38.55	-0.02

Notably, Rn was calculated as a function of the LAI, leaf angle distribution, radiation interception, and plant and soil reflectance. A robust LSM (Pollard and Thompson, 1995; Thompson and Pollard, 1995a, 1995b) supports biophysics process of Rn, e.g., the surface components of reflectance and transmittances that are used in simulation. As observed, the model efficiently simulated the Rn along the times series for both the sites, while following the periods of the presence and absence of green leaves.

Evapotranspiration (ET) is a function of the stomatal conductance and internal concentration of CO_2. The BBL model modified by Cuadra et al. (2021) account for stomatal opening at low water-vapor concentration, which is suitable for developing the simulations for sugarcane, as it is a semi-perennial plant (with approximately 12 months of growing season), and thus, is exposed to the critical values of vapor pressure deficit (VPD) throughout the year, especially in dry season in a tropical savanna environment.

Regarding carbon assimilation, NEE is an important diagnostic variable that integrates GPP and ecosystem respiration (Re). In this study, NEE fluctuation was observed along the times series; it varied as a function of plant growth and harvest time, wherein negative balance indicated greater CO_2 assimilation by the ecosystem from the atmosphere and thus, a higher metabolic activity. The periods with a positive balance indicate CO_2 losses to the atmosphere, occurring predominantly in the harvest and/or post-harvest periods. For both the sites, the model captured the fluctuations of the NEE along the season. The NEE is the difference between GPP and Re. The Re accounts for autotrophic and soil heterotrophic respirations, which were computed in the LSM and biogeochemical modules, respectively.

Although the LOESS algorithm indicated that the simulated and observed data (Figs. 4 and 5) were similar along the times series for the NEE, we noted low values of NSE (observed in Table 2) for both the sites (sites 1 and 2). However, the values were positive, indicating that the model simulations were more reliable that the historical observed data. Low values of NSE can be explained by a high disparity between the observed and simulated values of NEE along the times series, which may increase the variance and consequently reduce the NSE. The simulation of GPP responded consistently to temperature and humidity for both the sites (Figs. 4 and 5). However, an overestimation was observed for 15–32 °C and 25–80% of humidity for site 1 (Fig. 4). The GPP simulation

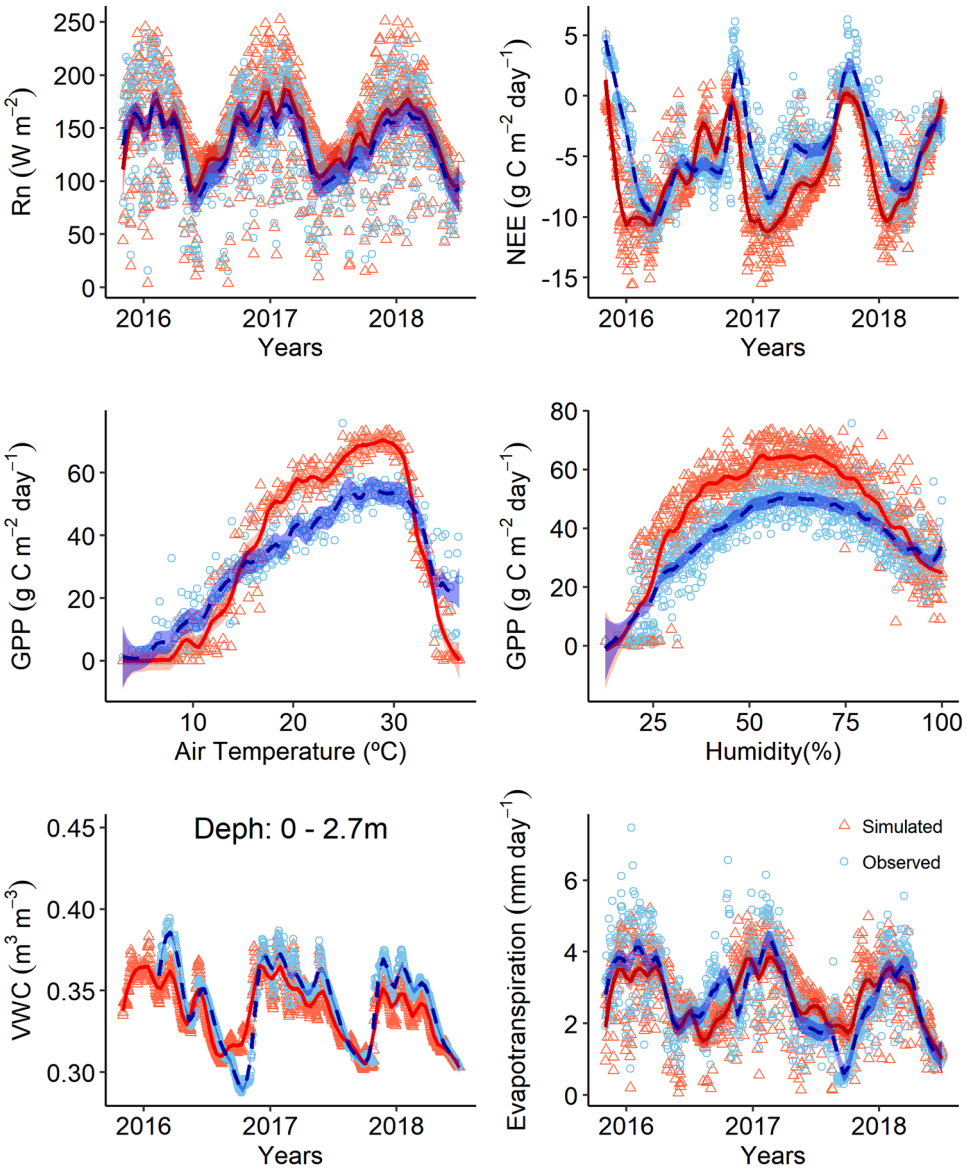

Fig. 4. Simulated and observed daily mean total net radiation (Rn), net ecosystem exchange (NEE), gross primary production (GPP) vs temperature (C°) and humidity (%), daily total evapotranspiration (ET) and volumetric water content (VWC) for Site 1, based on Dataset 1. Blue triangles and red circles denote to the observed and simulated values, respectively. Dashed and solid lines represent the results of nonparametric local regression (LOESS), with 95% confidence interval.

for Site 2 (Fig. 5) was more accurate than that for Site 1. For Site 1, the observed values did not exceed 60 μmol CO_2 m^{-2} s^{-1} for 15–30 °C and 40–80% of humidity, however; for site 2, the value exceeded. A comparison of the simulated and observed GPP for Site 2 revealed an overlap throughout the time series, indicating a consistency of the model (with respect to physiological equations).

Additionally, the observed and simulated data portrayed lower abrupt intra-seasonal fluctuations throughout the time series, driven by short-term water deficit. The periods of higher water deficit can be diagnosticated using VWC and PAW (shown in Figs. 4–6). Water availability for plants is a critical factor for physiological processes. A water deficit will reduce the stomata opening, due to the higher vapor pressure deficit, leading to lower ET. Consequently, a reduction in the photosynthesis rate will lower the net exchange with the environment. This also explains the lower NEE values observed for the periods of lower VWC and PAW. Therefore, high accuracy in soil water prediction is critical for modeling the biophysical processes of crops.

Statistically (Table 2) and graphically (Fig. 6), throughout the time series, the simulated PAW values (calculated using Richard's equations) were similar to the observed ones for both the saturated and unsaturated water flows along the entire soil profile. The soil water model accurately simulated a higher and lower amount of water in the wet and dry seasons, respectively, thus, following the climate seasonality (Figs. 4 and 5).

The stalk and leaf biomasses were simulated consistently (Table 2 and Fig. 7), despite the differences in genotypes, crop management, and plant ages between sites 1 and 2. The evaluated dataset from Site 1 was based on the growing year and two consecutive ratoons, and that of Site 2 was based on the second and third ratoons. The parametrization from Site 1 was applied to Site 2, but the parameters of specific leaf area and root density were recalibrated, to better express the behavior of the genotypes grown in Site 2, as the morphological characteristics of the crop can vary significantly between different genotypes. However, a slight underestimation was observed for the growing year for Site 1 and the 2nd ratoon for Site 2, and an overestimation was noted in the 3rd ratoon for Site 2.

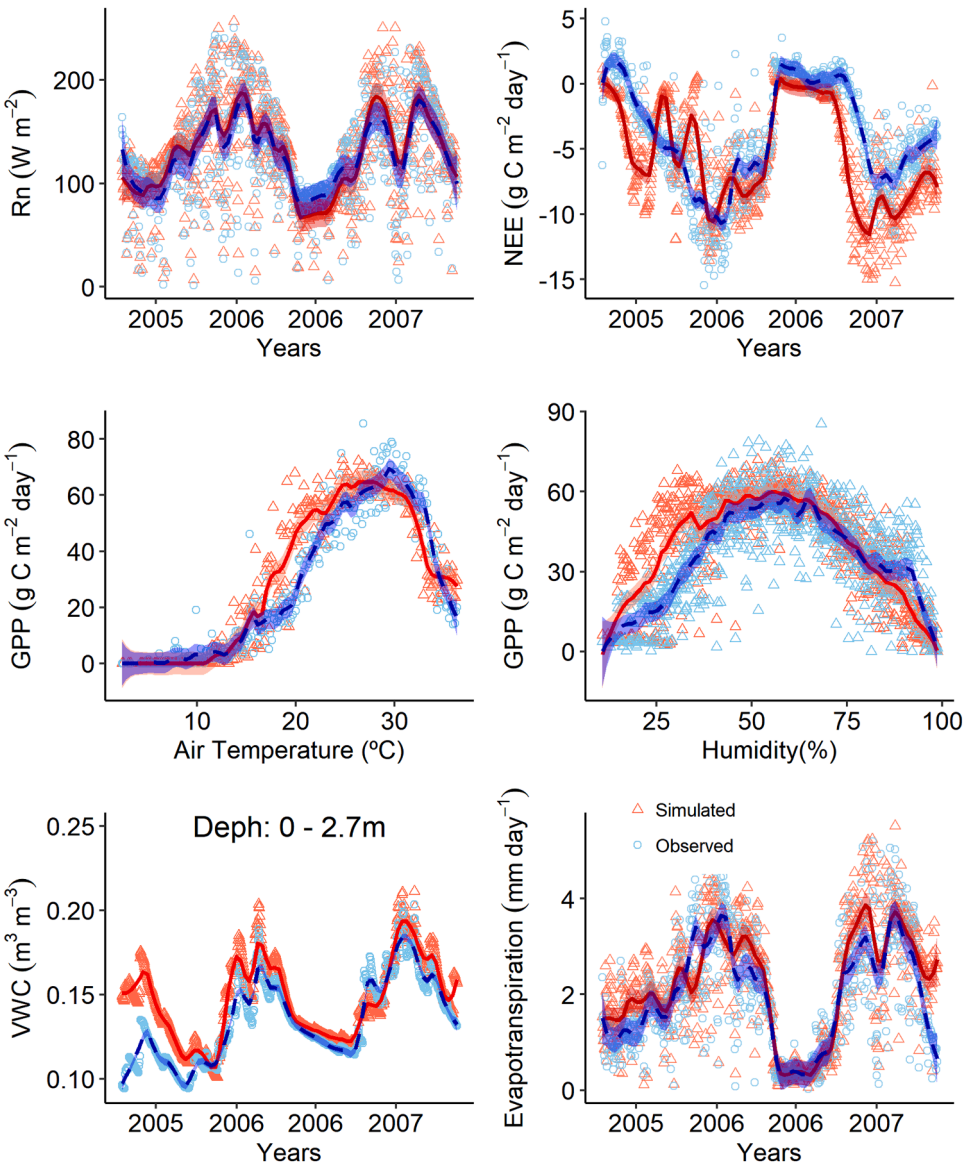

Fig. 5. Simulated and observed daily mean total net radiation (Rn), net ecosystem exchange (NEE), gross primary production (GPP) vs temperature (C°) and humidity (%), daily total evapotranspiration (ET), and volumetric water content (VWC) for Site 2, based on Dataset 2. Blue triangles and red circles correspond to the observed and simulated values, respectively. Dashed and solid lines represent the results for nonparametric local regression (LOESS), with 95% confidence interval.

3.2. Performance of ECOSystem MOdel Simulator (ECOSMOS)-sugarcane model: Calibration for early and mid-to-late harvest season genotypes

The simplified classification of sugarcane varieties into two groups, EMG and MLMG, provides a better distribution of genotypes across the edaphic and climatic gradients at Dataset 2. This approach provides greater model robustness for the calibration and evaluation procedures. We used one subset for calibration and another for evaluation.

As shown in Table 3 and Fig. 8, the statistics portrayed high performance (high NSE and low RRMSE and MB) in simulating the stalk biomass. For leaf biomass (not graphically represented) and LAI simulations, we noted a lw performance (low NSE and high RRMSE and MB). The results corresponded to the values of leaf biomass and LAI across the dataset. Different genotypes present different leaf characteristics; this may have contributed to the higher variability of the observed LAIs between the sites.

Regarding crop yield, the t-test and Wilcoxon signed-rank test did not portray statistical differences between the early and mid-to-late maturity genotype groups (p values of 0.2688 and 0.3692, respectively) indicating that, for the calibration dataset in each group, the means of the simulated and observed yields were not statistically different. This was consistent with the evaluation dataset for the early and mid-to-late maturity genotype groups with the p values 0.674 and 0.5212, respectively.

Compared to using the specie parameter set to simulate the two subsets from Dataset 2 (results are shown in Table S2 of Supplementary Material), we observed better performance when using the generic calibration approach to simulate the crop stalk. For subset 1, we noted an increase in the NSE from 0.80 to 0.82 and a reduction in the RRMSE from 44.08 to 41.76. For subset 2, we noted an increase in the NSE from 0.85 to 0.9 and a reduction in the RRMSE from 41.66 to 34.96. Regarding the yields of all the field plots, a statistical significance was observed for the mid-to-late harvest season group of subset 2 (Fig. S1 of Supplementary Material), indicating that the means of the simulated and observed data were not consistent; however, when applying the generic calibration approach, they were consistent (Fig. 8F).

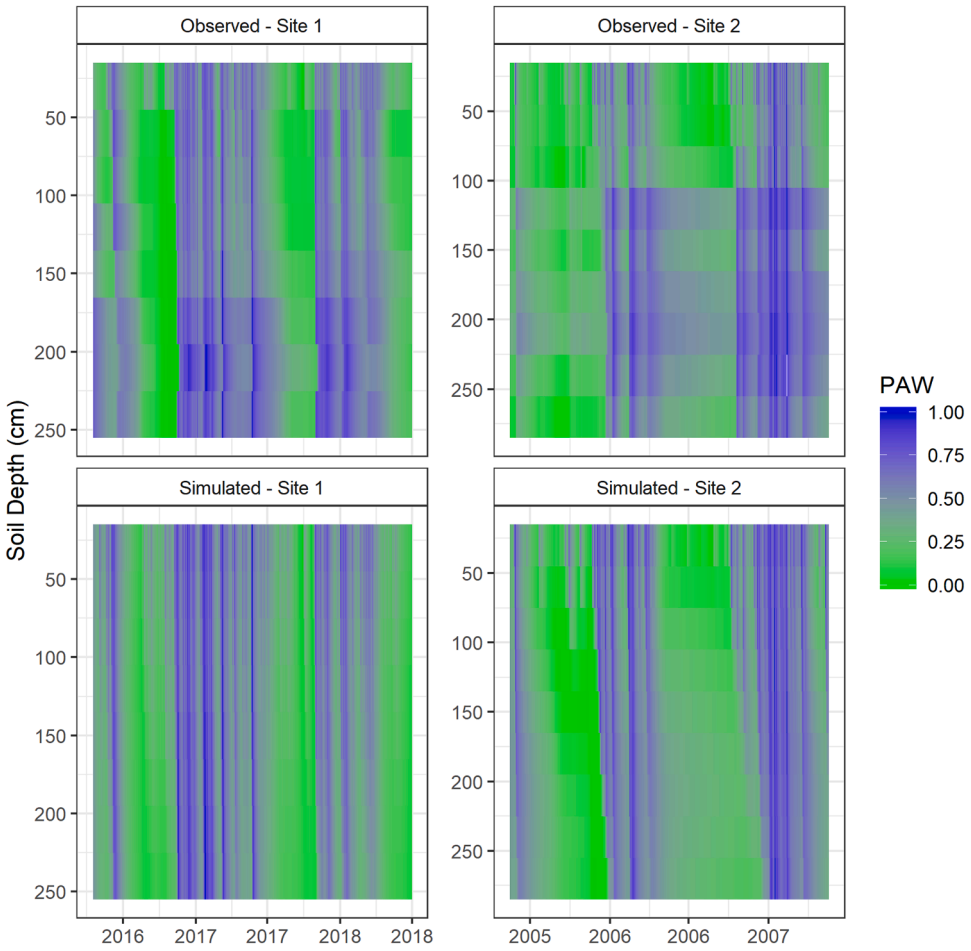

Fig. 6. Normalized plant available water (PAW) along the soil depth. The range varies from 0 to 1, where 0 indicates no water availability and 1 indicates maximum water availability. The column on the left corresponds to the observed and simulated PAW values for Site 1, and those on the right correspond to the observed and simulated PAW values for Site 2.

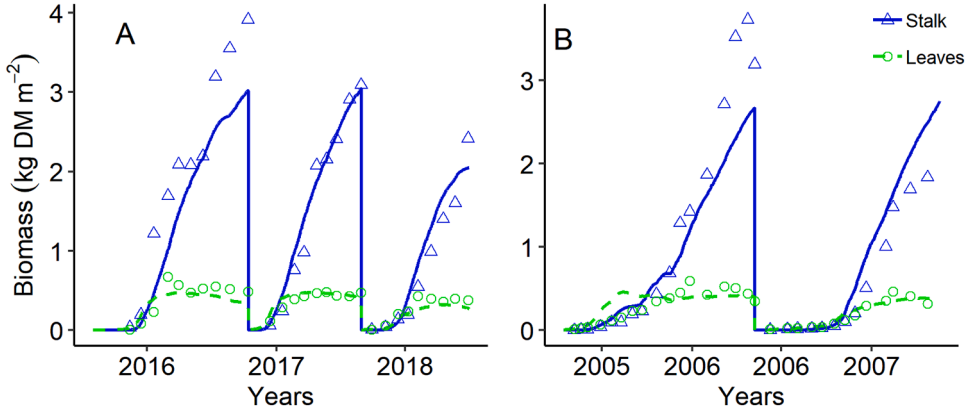

Fig. 7. Simulated and observed dry matter for experimental sites 1 (Fig. A) and 2 (Fig. B), based on Dataset 1. Solid and dash lines denote the simulated values for the crop stalk and leaves, respectively; blue triangles and green circles denote the observed values for stalk and leaves, respectively.

3.3. Yield estimation for sugarcane fields plots

The t-test and Wilcoxon signed-rank test (Fig. 9) indicated non-statistical significance differences between the observed and simulated yields only for the production environment A (i.e., no difference was noted between the mean observed and simulated values). For production environments B, C, D, and E, we noted statistical significance differences between the mean observed and simulated values, indicating that the model could not efficiently simulate the yields of these production environments. The difference between the means of the observed and simulated yields (absolute values) of the field plots were 0.9, 14.5, 2.9, 7.5, and 1.8 Mg ha^{-1} for production environments A, B, C, D, and E, respectively.

To increase the accuracy of the ECOSMOS-sugarcane module with respect to simulating the yields of the field plots, a "farm calibration" was proposed, wherein a subset is used for calibration and a second

Table 3
Performance of the ECOSystem MOdel Simulator (ECOSMOS)-sugarcane module for generic calibration of different variables for the two subsets, based on Dataset 2. Abbreviations: Leaf area index (LAI); dry matter (DM); Nash-Sutcliffe efficiency (NSE); relative root mean square error (RRMSE); mean bias (MB).

Dataset	Site	Calibration/ evaluation	Variables	Units	NSE	RRMSE	MB
2	3 to 20	Calibration (subset 1)	Stalk	kg DM m^{-2}	0.82	41.76	0.24
			Leaves	kg DM m^{-2}	-0.17	136.54	-0.33
			LAI	m^2 m^{-2}	-1.74	67.23	-1.87
		Evaluation (subset 2)	Stalk	kg DM m^{-2}	0.90	34.96	0.12
			Leaves	kg DM m^{-2}	0.09	191.76	-0.04
			LAI	m^2 m^{-2}	-1.99	67.69	-2.00

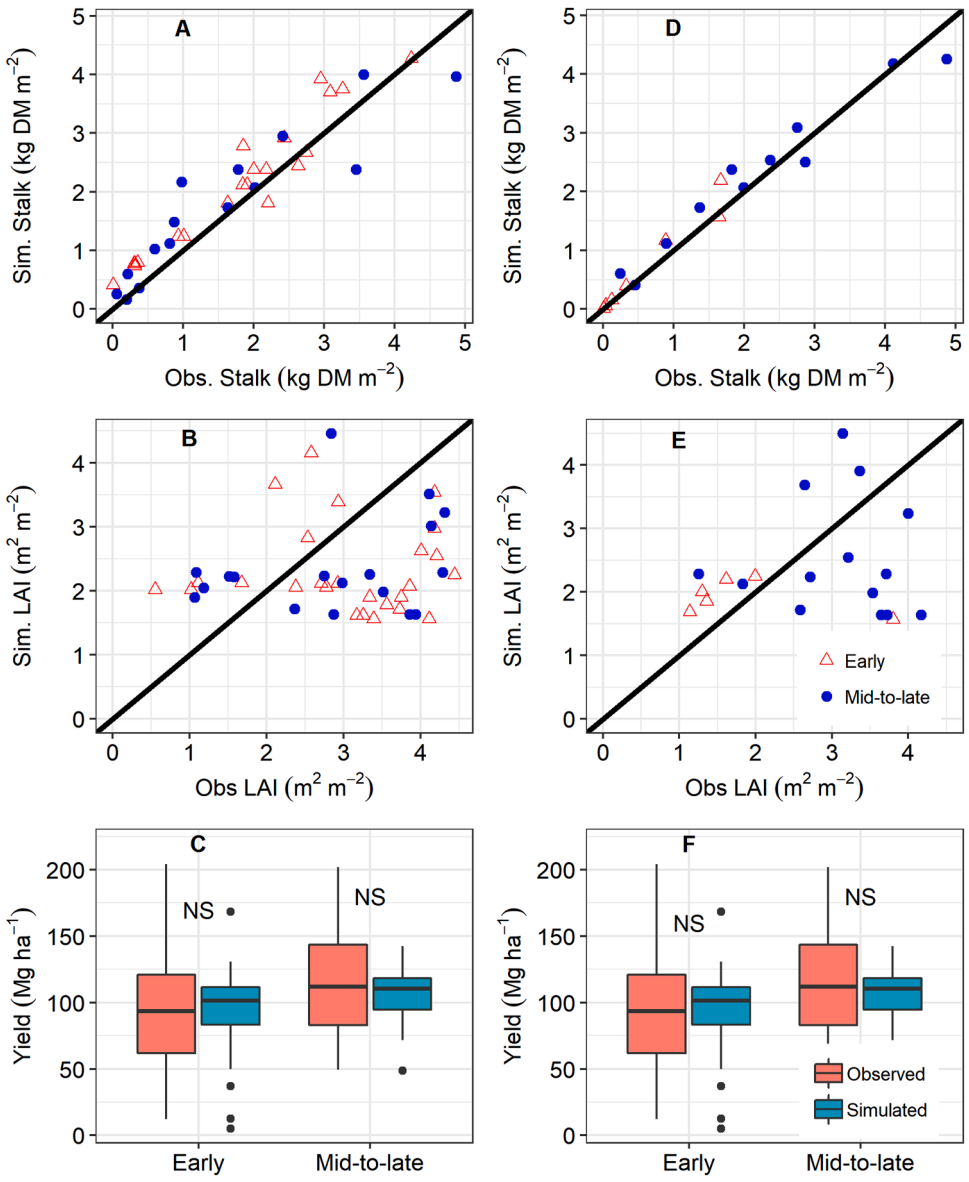

Fig. 8. Simulated and observed stalk, leaf area index (LAI) and Yield in sites 3 – 20 of dataset 2 used to calibrate (columns on the left, Fig. A, B, and C), and to evaluate (columns on the right, Fig. D, E, and F) the ECOSMOS-Sugarcane parameters set as early and mid-to-late maturity genotypes. "NS" indicates non-statistical significance between the observed and simulated values for yield (Mg ha^{-1}).

subset is used for evaluation. This calibration was based on production environment B, and the novel parameter set of production environment B was applied for the other production environments as well; however, in such scenarios, the rooting zone was penalized (see Section 2.3). The non-statistical significance indicated that the simulated and observed data were similar for all the production environments in the dataset used for calibration (Fig. 10A) and evaluation (Fig. 10B). The difference between the means of the observed and simulated yields (absolute values) of the field plots were 0.3, 1.6, 1.8, 2.2, and 0.4 Mg ha^{-1} for the production environments A, B, C, D, and E, respectively, of subset 2.

4. Discussion

The Rn calculated using the land surface module (Pollard and

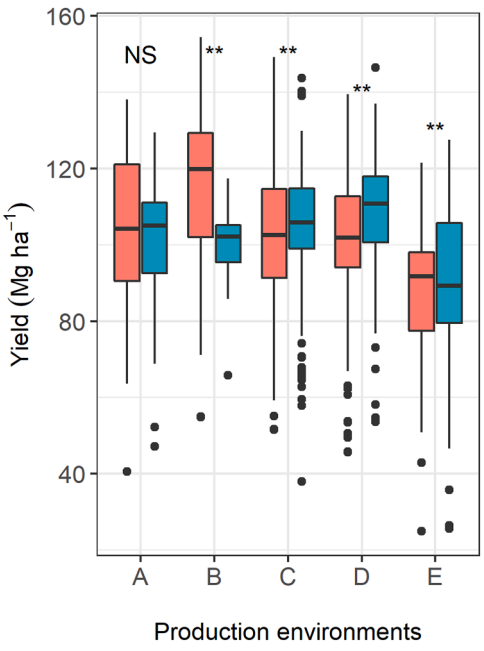

Fig. 9. Simulated and observed stalk (Mg ha^{-1}) for Dataset 3 used to evaluate the ECOSystem MOdel Simulator (ECOSMOS)-sugarcane parameters sets for the early and mid-to-late harvest seasons in field plots varying the production environments (Dataset 3). "* *" and "NS" indicate the statistical ($P < 0.05$) and non-statistical ($P \geq 0.05$) significances, respectively, between the observed and simulated values of yield (Mg ha^{-1}) (for each production environments).

Thompson, 1995; Thompson and Pollard, 1995a, 1995b), ET calculated using the BBL model modified by Cuadra et al. (2021), and soil water (VWC and PAW) calculated using Richard's equations were simulated efficiently throughout the time series. In particular, the GPP at the leaf scale was regulated by light, intercellular CO_2 concentration, and the Rubisco regeneration rate (Farquhar et al., 1980). In this study, the maximum Rubisco carboxylation was set up for the air temperature of 5–38 °C, regulated by the parameters explained in Supplemental Material Table S1. This range of temperatures regulates the plant metabolic activity (in this case, expressed by the GPP), with a suboptimal metabolic activity noted below approximately 15 °C. The optimal values were noted for 25–32 °C, and an abrupt reduction was noted above ~30 °C (Figs. 4 and 5). The carboxylation of Rubisco as a function of the temperature is well-documented in the literature. In particular, sugarcane portrays optimal Rubisco carboxylation activity at 35 °C, with suboptimal activity below 10 °C and an abrupt drop observed above 42 °C (Vianna et al., 2022). However, a slight variation with the optimal activity was noted at 23–29 °C during the period of early plant development (Guerra et al., 2013).

Additionally, the module accurately simulated the GPP response to the variations in the relative humidity (RH); RH was used to compute the VPD at an hourly time scale. At low VPD, which refers to low humidity, we noted a reduction in the stomatal opening and consequently, transpiration and the photosynthesis rate. The accurate simulation of photosynthesis with respect to the threshold of metabolic activity, i.e., at high or low temperatures and humidity conditions (or VPD), is crucial for any crop model. Investigating the factors that impact GPP based on an extensive and global database, Bao et al. (2022) verified that VPD is the main driver for GPP in the tropics. Patel et al. (2021) highlighted that VPD is the most important variable after PAR, which directly affects the net CO_2 assimilation in sugarcane in the growing season. Besides VPD, temperature and precipitation are the main drivers that will determine the pattern of reduction in sugarcane yield for different climate scenario estimations for Brazil in the future (Flack-Prain et al., 2021).

Overall, sugarcane is an important crop in several countries, especially in Brazil, a country that is responsible for approximately a quarter of global sugar production and 50% of global export (Marin, 2016). Although the major sugarcane production regions are located at Southeast and Midwest Brazil (IBGE, 2022), known to have predominantly Cfa, Cfb, and Aw climates, sugarcane is cultivated in the majority of Brazilian states (Fig. S2). Furthermore, it is an important crop for the local economy of multiple countries; sugar and ethanol are the major sugarcane derivate products, and it is also used to produce distilled drinks, animal feed, biodiesel, bio-electricity, biobutanol, chemicals (butanediol and biopolymers), several types of enzymes, and organic

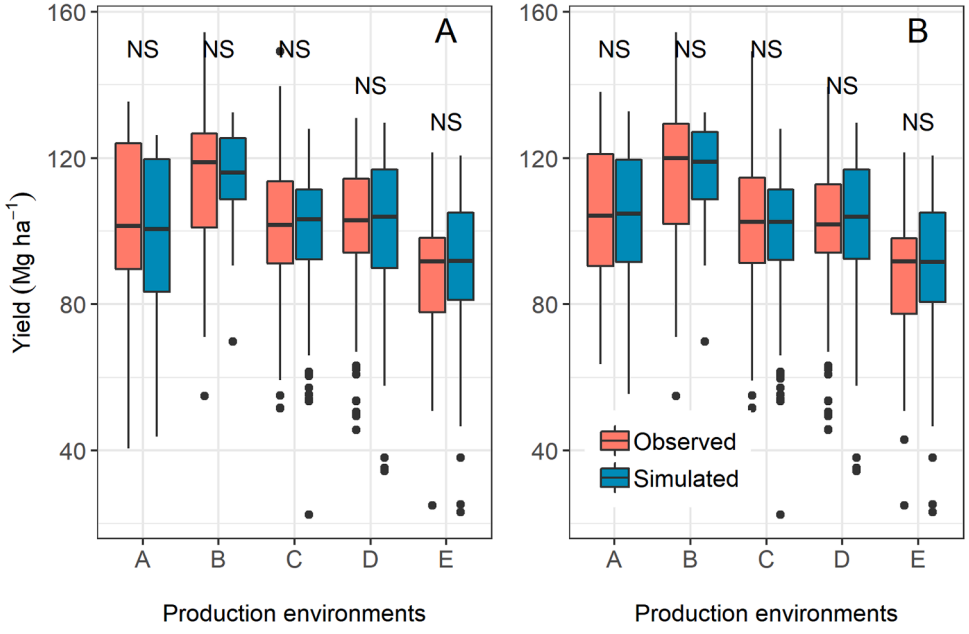

Fig. 10. Simulated and observed stalk (Mg ha^{-1}) for two subsets of Dataset 3 (field plots). The left panel (A) represents the subset used to calibrate the ECOSystem MOdel Simulator (ECOSMOS)-sugarcane parameters and the right panel (B) represents the subset used for evaluation. "NS" indicates non-statistical significance ($P \geq 0.05$) between the observed and simulated values for the stalk (Mg ha^{-1}) for all the production environments (A–E).

acid products (Mohlala et al., 2016; Sindhu et al., 2016). Therefore, accurately modeling sugarcane growth and yield across different environmental conditions has implications for several sectors.

Although sugarcane modeling has been extensively used to investigate the current and future sugarcane production in different scenarios of climate change in several countries (e.g., Brazil, India, Australia, and South Africa), the calibrations and model evaluations in previous studies were carried out based on limited data, generally with less than 10 experimental sites (e.g., Dias et al., 2019, 2021; Hoffman et al., 2018; Jones and Singels, 2018; Peng et al., 2020; Singels et al., 2014) and rarely with more than ten experimental sites (e.g., Dias and Sentelhas, 2017; Verma et al., 2023; Vianna et al., 2022). Notably, the majority of these studies were caried out in specific climate and soil conditions. In this study, the ECOSMOS-sugarcane model was calibrated and evaluated based on a dataset that contained 18 agrometeorological experiments carried out in contrasting environments and encompassing 22 varieties (Dataset 2), which portrayed significant GxE variability.

Despite the high performance of the sugarcane module simulation of the experimental sites, the sugarcane yields for the commercial field plots could not be predicted accurately (Fig. 9). However, this was not totally unexpected, as the performance of the sugarcane field plots were driven not only by the plant's response to the environmental production, but by the farmer's management practices and technology adopted in the sites also. For example, the observed yield was higher for environment B than environment A (which was the environment that had the highest productivity potential), thus, portraying contrast. As shown in Table 1, we noted a clay-content gradient from production environments A to E. The clay content and other soil properties (e.g., bulk density, total porosity, field capacity, and permanent wilting point) were responsible for soil-water infiltration, flux, retention, and availability. Theoretically, the greater the amount of available water, the greater the yield of the plant; however, we observed a higher yield for production environment B. Furthermore, we speculated a lack of pattern of decreasing yield from production environments A to E, resulting from some particularities in the management practices, e.g., soil preparation, fertilization, harvest time, vigor in regrowth, and difference in the performance of genotypes. This phenomenon might have influenced the local yield, leading to an unpredictability between the environments (as those factors are rarely quantified and thus, not represented in the model).

The gradual phasing out of pre-harvest burning and manual harvest, replaced by mechanical harvesting, also posed different challenges. The use of heavy machinery for harvesting sugarcane at the beginning and end of the cropping season, coinciding with the end and beginning of the rainy season, respectively, over successive years (de Lima et al., 2021), might be critical for soil compaction, a reduction in soil porosity (Toledo et al., 2021), infiltration rate, and root development, especially in clay soils. The management strategy generally used to withstand drought is to harvest production environments with lower soil-water retention capacity (production environments D and E) at the beginning of the season (when there is less water deficit). In such cases, the optimal environment (production environment A) is harvested at the end of the season. However, if the onset of the subsequent rainy season is early, the environments with the highest clay content (with the soil having excessive moisture content) are harvested first. Notably, this approach accentuates the problem of soil compaction and may even lead to plant shock effects and stump uprooting, thus, reducing the plant population and yield in the next harvest. Even soils with thicker straw blankets, accumulated throughout several ratoons with non-burn mechanical harvesting, cannot avoid the risk of soil compaction (Cherubin et al., 2021).

To manage water stress, the main driver of yield loss and best fertilizers and irrigation practices can be prioritized to ensure a more controlled production environment, thus, setting a crop management bias that reduces the actual difference in the yield potential across the production environments. Using large datasets from actual production fields improves modeling, but requires adjustments in crop management practices by farmers, posing severe challenges for accurate modeling. Therefore, we propose the hypothesis that mechanization (and not less favorable soil water conditions) is leading to more yield loss in production environment A (in comparison to that in production environment B), which was not consistently simulated by the module in the first simulation.

Therefore, we propose a farm-level calibration to increase model accuracy, once the management techniques, genotype performances, and interactions of different genotypes with the environment were analyzed with respect to their implications for crop growth and yield. This approach has improved the model accuracy for different crops (Colmanetti et al., 2022; Therond et al., 2011). In this study, only two parameters were calibrated using the production environment B as reference; for the other production environments (A, C, D, and E), the rooting zone was penalized. The accumulated root density was reduced to a depth of 60 cm for production environment C and 40 cm for production environments D and E. This approach was successful for this study and was based on Zhao et al. (2020), wherein the majority of roots (~80%) were in the superficial layers (~50 cm).

Although sugarcane plays an important role for economy, the sugarcane sector has experienced several challenges in the last few decades. Notably, in Brazil, some issues have limited the increase in the yield, e.g., demand of breeding programs for focusing on novel varieties adapted to new arable areas, yield decline as a consequence of soil compaction and the mechanical damage to the crop ratoons, limited improvement in agronomic management, non-upgrades on mechanical no-till planting, and the lack of improvements in planning, management practices, and yield prediction (Marin, 2016). All these challenges intensify with climate change. In this context, sugarcane modeling based on ECOSMOS can support: (i) the planning, i.e., determine the ideal period for planting or harvesting in a specific season, especially in novel arable areas where sugarcane is not traditionally planted and identify arable areas that can be potentially used for sugarcane plantation. (ii) Yield prediction, i.e., crop modeling can be used to simulate the sugarcane yield in different locations in any hypothetical climate scenario.

Additionally, with the increased demand for food, fiber, and biofuels, in the future, the agricultural sector will face enormous challenges related to sustainable development, which combines issues related to the economic, ecological, and human spheres. The achievement of global food and energy security is conditioned by the reduction of negative ecological impacts and improvements in environmental benefits, e.g., the mitigation of GHG emissions. For the specific case of sugarcane cultivation in Brazil, the recent expansion of sugarcane plantations in the last few decades occurred in degraded pastures, potentially providing environmental benefits, such as enhancing the C budget in soil (Bordonal et al., 2018). The results presented in this study demonstrate the effectiveness of the ECOSMOS-sugarcane model in simulating water and carbon balances and sugarcane growth and yield in tropical environments. Therefore, ECOSMOS can be applied, for example, to evaluate the trade-offs of agriculture production and assess the impacts on ecosystem goods-and-services (e.g., carbon storage and hydrology) (Anderson-Teixeira et al., 2012; O'Connell et al., 2018).

5. Conclusion

The parametrization (specie parametrization) process carried out for Site 1, while considering the carbon flux, Rn, ET, soil water content, biomass, and yield, was successfully evaluated for Site 2, with the NSE values being 0.14–0.86 and RRMSE values, 13–112.

A generic calibration carried out using a dataset of agrometeorological experiments with high GxExM variability performed satisfactorily in predicting crop yield. As the generic calibration was performed for different climates and soil textures, it can be used as a reference for other sites in Brazil that have same climate conditions. However, this calibration performed poorly when estimating the yield for a specific farm. Alternatively, a farm calibration was performed to

enhance the accuracy of the yield, and it was consistent between the simulated and observed field plots, for all the five production environments. This approach has been proven to be a feasible alternative to incorporate local management practices, such as soil preparation, fertilization, harvest time, vigor in regrowth, and the differences in the performance of genotype practices into the parameters set.

The ECOSMOS-Sugarcane module can be applied as a tool to better understand the effects of sugarcane plantations on carbon sequestration and water resources and predict sugarcane growth and yield in tropical environments. Additionally, ECOSMOS allows the simulation of two canopy levels and more than one crop per level. Therefore, the ECOSMOS-sugarcane module can also be applied to evaluate the impacts and commercial benefits of sugarcane production in monocropping, intercropping, and crop-rotation systems, especially in Brazil where all these agricultural systems are widely adopted.

CRediT authorship contribution statement

Marafon Anderson Carlos: Data curation, Writing – original draft. **de Andrade Junior Aderson Soares:** Data curation, Writing – original draft. **Galdos Marcelo Valadares:** Conceptualization, Funding acquisition, Writing – original draft. **Monteiro José Eduardo Boffino de Almeida:** Investigation, Writing – original draft. **de Freitas Helber Custódio:** Data curation, Writing – original draft. **Cabral Osvaldo Machado Rodrigues:** Data curation, Methodology, Writing – original draft. **Victoria Daniel de Castro:** Formal analysis, Software, Writing – original draft. **Hernandes Thayse Aparecida Dourado:** Data curation, Writing – original draft, Writing – review & editing. **Cuadra Santiago Vianna:** Conceptualization, Data curation, Formal analysis, Methodology, Software, Supervision, Validation, Visualization, Writing – original draft, Writing – review & editing. **le Maire Guerric:** Conceptualization, Formal analysis, Investigation, Methodology, Validation, Writing – original draft, Writing – review & editing. **Lamparelli Rubens Augusto Camargo:** Conceptualization, Funding acquisition, Project administration, Writing – original draft, Writing – review & editing, Resources, Supervision. **Silva Sergio Delmar dos Anjos e:** Data curation, Writing – original draft. **Bufon Vinicius Bof:** Data curation, Validation, Writing – original draft, Writing – review & editing. **Colmanetti Michel Anderson Almeida:** Conceptualization, Formal analysis, Investigation, Methodology, Software, Validation, Visualization, Writing – original draft, Writing – review & editing.

Declaration of Competing Interest

The authors declare that they have no known competing financial interests or personal relationships that could have appeared to influence the work reported in this paper.

Data Availability

The authors do not have permission to share data.

Acknowledgements

This work was supported by the FAPESP-Microsoft Research project “Characterizing and Predicting Biomass Production in Sugarcane and Eucalyptus Plantations in Brazil” (SEMP) of the São Paulo Research Foundation (FAPESP-Microsoft Research no. 2014/50715-9). Michel A. A. Colmanetti was supported by a post-doctoral grant (grant no. 2018/21103-6) from the Sao Paulo Research Foundation (FAPESP).

Appendix A. Supporting information

Supplementary data associated with this article can be found in the online version at doi:10.1016/j.eja.2023.127061.

References

Alvares, C.A., Stape, J.L., Sentelhas, P.C., De Moraes Gonçalves, J.L., Sparovek, G., 2013. Köppen’s climate classification map for Brazil. Meteorol. Z. 22, 711–728. https://doi.org/10.1127/0941-2948/2013/0507.

Anderson-Teixeira, K.J., Snyder, P.K., Twine, T.E., Cuadra, S.V., Costa, M.H., DeLucia, E. H., 2012. Climate-regulation services of natural and agricultural ecoregions of the Americas. Nat. Clim. Chang. 2, 177–181. https://doi.org/10.1038/nclimate1346.

Ball-Coelho, B., Sampaio, E.V.S.B., Tiessen, H., Stewart, J.W.B., 1992. Root dynamics in plant and ratoon crops of sugar cane. Plant Soil 142, 297–305. https://doi.org/10.1007/BF00010975.

Bao, S., Wutzler, T., Koirala, S., Cuntz, M., Ibrom, A., Besnard, S., Walther, S., Šigut, L., Moreno, A., Weber, U., Wohlfahrt, G., Cleverly, J., Migliavacca, M., Woodgate, W., Merbold, L., Veenendaal, E., Carvalhais, N., 2022. Environment-sensitivity functions for gross primary productivity in light use efficiency models. Agric. . Meteorol. 312 https://doi.org/10.1016/j.agrformet.2021.108708.

Barbosa, A., de, M., Zilliani, R.R., Tiritan, C.S., Souza, G.M., Silva, M., de, A., 2021. Energy conversion efficiency in sugarcane cultivars as a function of production environments in Brazil. Renew. Sustain. Energy Rev. 150 https://doi.org/10.1016/j.rser.2021.111500.

Benezoli, V.H., Imbuzeiro, H.M.A., Cuadra, S.V., Colmanetti, M.A.A., de Araújo, A.C., Stiegler, C., Motoike, S.Y., 2021. Modeling oil palm crop for Brazilian climate conditions. Agric. Syst. 190 https://doi.org/10.1016/j.agsy.2021.103130.

Bordonal, R., de, O., Carvalho, J.L.N., Lal, R., de Figueiredo, E.B., de Oliveira, B.G., La Scala, N., 2018. Sustainability of sugarcane production in Brazil. A review. Agron. Sustain. Dev. 38 https://doi.org/10.1007/s13593-018-0490-x.

Cabral, O.M.R., Rocha, H.R., Gash, J.H., Ligo, M.A.V., Tatsch, J.D., Freitas, H.C., Brasilio, E., 2012. Water use in a sugarcane plantation. GCB Bioenergy 4, 555–565. https://doi.org/10.1111/j.1757-1707.2011.01155.x.

Cabral, O.M.R., Rocha, H.R., Gash, J.H., Ligo, M.A.V., Ramos, N.P., Packer, A.P., Batista, E.R., 2013. Fluxes of CO_2 above a sugarcane plantation in Brazil. Agric. . Meteorol. 182–183, 54–66. https://doi.org/10.1016/j.agrformet.2013.08.004.

Cabral, O.M.R., Freitas, H.C., Cuadra, S.V., de Andrade, C.A., Ramos, N.P., Grutzmacher, P., Galdos, M., Packer, A.P.C., da Rocha, H.R., Rossi, P., 2020. The sustainability of a sugarcane plantation in Brazil assessed by the eddy covariance fluxes of greenhouse gases, 107864 Agric. . Meteorol. 282–283. https://doi.org/10.1016/j.agrformet.2019.107864.

Cherubin, M.R., Franchi, M.R.A., Lima, R.P. de, Moraes, M.T. de, Luz, F.B. da, 2021. Sugarcane straw effects on soil compaction susceptibility. Soil Tillage Res 212, 105066. https://doi.org/10.1016/j.still.2021.105066.

Colmanetti, M.A.A., Cuadra, S.V., Lamparelli, R.A.C., Bortolucci Júnior, J., Cabral, O.M. R., Campoe, O.C., Victoria, D. de C., Barioni, L.G., Galdos, M.V., Figueiredo, G.K.D. A., Maire, G. le, 2022. Implementation and calibration of short-rotation eucalypt plantation module within the ECOSMOS land surface model. Agric. . Meteorol. 323 https://doi.org/10.1016/j.agrformet.2022.109043.

Cuadra, S.V., Costa, M.H., Kucharick, C.J., Da Rocha, H.R., Tatsch, J.D., Inman-Bamber, G., Da Rocha, R.P., Leite, C.C., Cabral, O.M.R., 2012. A biophysical model of Sugarcane growth. GCB Bioenergy 4, 36–48. https://doi.org/10.1111/j.1757-1707.2011.01105.x.

Cuadra, S.V., Kimball, B.A., Boote, K.J., Suyker, A.E., Pickering, N., 2021. Energy balance in the DSSAT-CSM-CROPGRO model. Agric. . Meteorol. 297, 108241 https://doi.org/10.1016/j.agrformet.2020.108241.

Daioglou, V., Doelman, J.C., Wicke, B., Faaij, A., van Vuuren, D.P., 2019. Integrated assessment of biomass supply and demand in climate change mitigation scenarios. Glob. Environ. Chang. 54, 88–101. https://doi.org/10.1016/j.gloenvcha.2018.11.012.

Daioglou, V., Muratori, M., Lamers, P., Fujimori, S., Kitous, A., Köberle, A.C., Bauer, N., Junginger, M., Kato, E., Leblanc, F., Mima, S., Wise, M., van Vuuren, D.P., 2020. Implications of climate change mitigation strategies on international bioenergy trade. Clim. Change 163, 1639–1658. https://doi.org/10.1007/s10584-020-02877-1.

Dias, H.B., Sentelhas, P.C., 2017. Evaluation of three sugarcane simulation models and their ensemble for yield estimation in commercially managed fi elds. F. Crop. Res. 213, 174–185. https://doi.org/10.1016/j.fcr.2017.07.022.

Dias, H.B., Inman-Bamber, G., Bermejo, R., Sentelhas, P.C., Christodoulou, D., 2019. New APSIM-Sugar features and parameters required to account for high sugarcane yields in tropical environments. F. Crop. Res. 235, 38–53. https://doi.org/10.1016/j.fcr.2019.02.002.

Dias, H.B., Inman-Bamber, G., Sentelhas, P.C., Everingham, Y., Bermejo, R., Christodoulou, D., 2021. High-yielding sugarcane in tropical Brazil – Integrating field experimentation and modelling approach for assessing variety performances. F. Crop. Res. 274 https://doi.org/10.1016/j.fcr.2021.108323.

Dias, H.B., Cuadra, S.V., Boote, K.J., Lamparelli, R.A.C., Figueiredo, G.K.D.A., Suyker, A. E., Magalhães, P.S.G., Hoogenboom, G., 2023. Coupling the CSM-CROPGRO-Soybean crop model with the ECOSMOS Ecosystem Model – An evaluation with data from an AmeriFlux site. Agric. . Meteorol. 342, 109697 https://doi.org/10.1016/j.agrformet.2023.109697.

Farquhar, G.D., von Caemmerer, S., Berry, J.A., 1980. A biochemical model of photosynthetic CO_2 assimilation in leaves of C3 species. Planta 149, 78–90. https://doi.org/10.1007/BF00386231.

Farthing, M.W., Ogden, F.L., 2017. Numerical Solution of Richards’ Equation: A Review of Advances and Challenges 1257–1269. https://doi.org/10.2136/sssaj2017.02.0058.

Flack-Prain, S., Shi, L., Zhu, P., da Rocha, H.R., Cabral, O., Hu, S., Williams, M., 2021. The impact of climate change and climate extremes on sugarcane production. GCB Bioenergy 13, 408–424. https://doi.org/10.1111/gcbb.12797.

Foley, J.A., Prentice, I.C., Ramankutty, N., Levis, S., Pollard, D., Sitch, S., Haxeltine, A., 1996. An integrated biosphere model of land surface processes, terrestrial carbon balance, and vegetation dynamics. Glob. Biogeochem. Cycles 10, 603–628. https://doi.org/10.1029/96GB02692.

Guerra, A., Barbosa, A., de, M., Guidorizi, K.A., Souza, G.M., 2013. Effects of air temperature on photosynthesis of sugarcane in the initial phase of its development. Rev. Agrar. 7, 211–217.

Hernandes, T.A.D., de Oliveira Bordonal, R., Duft, D.G., Leal, M.R.L.V., 2022. Implications of regional agricultural land use dynamics and deforestation associated with sugarcane expansion for soil carbon stocks in Brazil. Reg. Environ. Chang. 22, 49 https://doi.org/10.1007/s10113-022-01907-1.

Hoffman, N., Singels, A., Patton, A., Ramburan, S., 2018. Predicting genotypic differences in irrigated sugarcane yield using the Canegro model and independent trait parameter estimates. Eur. J. Agron. 96, 13–21. https://doi.org/10.1016/j.eja.2018.01.005.

IBGE, 2022. Tabela 1612 - Área plantada, área colhida, quantidade produzida, rendimento médio e valor da produção das lavouras temporárias [WWW Document]. URL ⟨https://sidra.ibge.gov.br/Tabela/1612⟩.

Jones, M.R., Singels, A., 2018. Refining the Canegro model for improved simulation of climate change impacts on sugarcane. Eur. J. Agron. 100, 76–86. https://doi.org/10.1016/j.eja.2017.12.009.

Junqueira, T.L., Chagas, M.F., Gouveia, V.L.R., Rezende, M.C.A.F., Watanabe, M.D.B., Jesus, C.D.F., Cavalett, O., Milanez, A.Y., Bonomi, A., 2017. Techno-economic analysis and climate change impacts of sugarcane biorefineries considering different time horizons. Biotechnol. Biofuels 10, 50. https://doi.org/10.1186/s13068-017-0722-3.

Keating, B., Robertson, M., Muchow, R., Huth, N., 1999. Modelling sugarcane production systems I. Development and performance of the sugarcane module. F. Crop. Res. 61, 253–271. https://doi.org/10.1016/S0378-4290(98)00167-1.

Kucharik, C.J., Brye, K.R., 2003. Integrated BIosphere Simulator (IBIS) Yield and Nitrate Loss Predictions for Wisconsin Maize Receiving Varied Amounts of Nitrogen Fertilizer. J. Environ. Qual. 32, 247–268. https://doi.org/10.2134/jeq2003.2470.

Kucharik, C.J., Foley, J.A., Delire, C., Fisher, V.A., Coe, M.T., Lenters, J.D., Young-Molling, C., Ramankutty, N., Norman, J.M., Gower, S.T., 2000. Testing the performance of a dynamic global ecosystem model: Water balance, carbon balance, and vegetation structure. Glob. Biogeochem. Cycles 14, 795–825. https://doi.org/10.1029/1999GB001138.

Leuning, R., 1995. A critical appraisal of a combined stomatal-photosynthesis model for C3 plants. Plant, Cell Environ. 18, 339–355. https://doi.org/10.1111/j.1365-3040.1995.tb00370.x.

de Lima, R.P., Rolim, M.M., Daniel, D. da, da Silva, A.R., Mendonça, E.A.S., 2021. Compressive properties and least limiting water range of plough layer and plough pan in sugarcane fields. Soil Use Manag 37, 533–544. https://doi.org/10.1111/sum.12601.

Marin, F.R., 2016. Understanding sugarcane production, Biofuels, and market volatility in Brazil—a research perspective. Outlook Agric. 45, 75–77. https://doi.org/10.1177/0030727016649802.

Miner, G.L., Bauerle, W.L., Baldocchi, D.D., 2017. Estimating the sensitivity of stomatal conductance to photosynthesis: a review. Plant Cell Environ. 40, 1214–1238. https://doi.org/10.1111/pce.12871.

Mohlala, L.M., Bodunrin, M.O., Awosusi, A.A., Daramola, M.O., Cele, N.P., Olubambi, P. A., 2016. Beneficiation of corncob and sugarcane bagasse for energy generation and materials development in Nigeria and South Africa: a short overview. Alex. Eng. J. 55, 3025–3036. https://doi.org/10.1016/j.aej.2016.05.014.

O'Connell, C.S., Carlson, K.M., Cuadra, S., Feeley, K.J., Gerber, J., West, P.C., Polasky, S., 2018. Balancing tradeoffs: Reconciling multiple environmental goals when ecosystem services vary regionally. Environ. Res. Lett. 13 https://doi.org/10.1088/1748-9326/aaafd8.

Patel, N.R., Pokhariyal, S., Chauhan, P., Dadhwal, V.K., 2021. Dynamics of CO_2 fluxes and controlling environmental factors in sugarcane (C4)–wheat (C3) ecosystem of dry sub-humid region in India. Int. J. Biometeorol. 65, 1069–1084. https://doi.org/10.1007/s00484-021-02088-y.

Peng, T., Fu, J., Jiang, D., Du, J., 2020. Simulation of the growth potential of sugarcane as an energy crop based on the APSIM model. Energies 13. https://doi.org/10.3390/en13092173.

Petrielli, G.P., Nogueira, G.P., Henzler, D., de, S., de Souza, N.R.D., Bruno, K.M.B., Luciano, A.C. dos S., le Maire, G., Hernandes, T.A.D., 2023. Integrating carbon footprint to spatialized modeling: The mitigation potential of sugarcane ethanol production in the Brazilian Center-South. Resour. Conserv. Recycl. 189 https://doi.org/10.1016/j.resconrec.2022.106725.

Pollard, D., Thompson, S.L., 1995. Use of a land-surface-transfer scheme (LSX) in a global climate model: the response to doubling stomatal resistance. Glob. Planet. Change 10, 129–161. https://doi.org/10.1016/0921-8181(94)00023-7.

R Core Team, 2020. R: A language and environment for statistical computing.

Scarpare, F.V., Leal, M.R.L.V., Victoria, R.L., 2015. The challenges of sugarcane ethanol in Brazil: Past, present and future. In: Dallemand, J.F., Hilbert, J.A., Monforti, F. (Eds.), The Challenges of Sugarcane Ethanol in Brazil: Past, Present and Future. Publications Office of the European Union, Luxembourg, p. 201. ⟨https://doi.org/10.2790/246697⟩.

Sindhu, R., Gnansounou, E., Binod, P., Pandey, A., 2016. Bioconversion of sugarcane crop residue for value added products – an overview. Renew. Energy 98, 203–215. https://doi.org/10.1016/j.renene.2016.02.057.

Singels, A., Bezuidenhout, C.N., 2002. A new method of simulating dry matter partitioning in the Canegro sugarcane model. F. Crop. Res. 78, 151–164. https://doi.org/10.1016/S0378-4290(02)00118-1.

Singels, A., Donaldson, R.A., Smit, M.A., 2005. Improving biomass production and partitioning in sugarcane: theory and practice. F. Crop. Res. 92, 291–303. https://doi.org/10.1016/j.fcr.2005.01.022.

Singels, A., Jones, M., Marin, F., Ruane, A., Thorburn, P., 2014. Predicting Climate Change Impacts on Sugarcane Production at Sites in Australia, Brazil and South Africa Using the Canegro Model. Sugar Tech. 16, 347–355. https://doi.org/10.1007/s12355-013-0274-1.

Souza, N.R.D. de, Duft, D.G., Bruno, K.M.B., Henzler, D. de S., Junqueira, T.L., Cavalett, O., Hernandes, T.A.D., 2021. Unraveling the potential of sugarcane electricity for climate change mitigation in Brazil. Resour. Conserv. Recycl. 175 https://doi.org/10.1016/j.resconrec.2021.105878.

Therond, O., Hengsdijk, H., Casellas, E., Wallach, D., Adam, M., Belhouchette, H., Oomen, R., Russell, G., Ewert, F., Bergez, J.-E., Janssen, S., Wery, J., Van Ittersum, M.K., 2011. Using a cropping system model at regional scale: Low-data approaches for crop management information and model calibration. Agric. Ecosyst. Environ. 142, 85–94. https://doi.org/10.1016/j.agee.2010.05.007.

Thompson, S.L., Pollard, D., 1995a. A global climate model (GENESIS) with a land-surface transfer scheme (LSX). Part II: CO_2 sensitivity. J. Clim. https://doi.org/10.1175/1520-0442(1995)008<1104:AGCMWA>2.0.CO;2.

Thompson, S.L., Pollard, D., 1995b. A global climate model (GENESIS) with a land-surface transfer scheme (LSX). Part I: present climate simulation. J. Clim. https://doi.org/10.1175/1520-0442(1995)008<0732:AGCMWA>2.0.CO;2.

Toledo, M.P.S., Rolim, M.M., de Lima, R.P., Cavalcanti, R.Q., Ortiz, P.F.S., Cherubin, M. R., 2021. Strength, swelling and compressibility of unsaturated sugarcane soils. Soil Tillage Res 212. https://doi.org/10.1016/j.still.2021.105072.

Tollefson, J., 2018. Can the world kick its fossil-fuel addiction fast enough? Nature 556, 422–425. https://doi.org/10.1038/d41586-018-04931-6.

Tomasella, J., Hodnett, M.G., 1997. Estimating unsaturated hydraulic conductivity of Brazilian soils using soil-water retention data. Soil Sci. 162, 703–712. https://doi.org/10.1097/00010694-199710000-00003.

Tomasella, J., Hodnett, M.G., Rossato, L., 2000. Pedotransfer functions for the estimation of soil water retention in Brazilian Soils. Soil Sci. Soc. Am. J. 64, 327–338. https://doi.org/10.2136/sssaj2000.641327x.

USDA-SCS, 1998. Part 630 - Hydrology, in: U.S. Department of Agriculture, S.C.S. (Ed.), National Engineering Handbook. Michigan State University, p. 79.

Verma, A.K., Garg, P.K., Prasad, K.S.H., Dadhwal, V.K., 2023. Variety-specific sugarcane yield simulations and climate change impacts on sugarcane yield using DSSAT-CSM-CANEGRO model. Agric. Water Manag. 275, 108034 https://doi.org/10.1016/j.agwat.2022.108034.

Vianna, M.S., Williams, K.W., Littleton, E.W., Cabral, O., Cerri, C.E.P., De Jong van Lier, Q., Marthews, T.R., Hayman, G., Zeri, M., Cuadra, S.V., Challinor, A.J., Marin, F.R., Galdos, M.V., 2022. Improving the representation of sugarcane crop in the Joint UK Land Environment Simulator (JULES) model for climate impact assessment. GCB Bioenergy 14, 1097–1116. https://doi.org/10.1111/gcbb.12989.

Xavier, A.C., Scanlon, B.R., King, C.W., Alves, A.I., 2022. New improved Brazilian daily weather gridded data (1961–2020). Int. J. Climatol. 42, 8390–8404. https://doi.org/10.1002/joc.7731.

Zhao, L., Yang, K., Zhao, P., Qin, W., Zhao, Y., Zhu, J., Zan, F., Zhao, J., Lu, X., Wu, C., Burner, D.M., Chen, X., Liu, J., 2020. Sugarcane root distribution and growth as affected by genotype and crop cycle. Bragantia 79, 192–202. https://doi.org/10.1590/1678-4499.20190407.